



## Guide for interpreting and reporting luminescence dating results

Shannon A Mahan, Tammy M Rittenour, Michelle S Nelson, Nina Ataei, Nathan Brown, Regina Dewitt, Julie Durcan, Mary Evans, James Feathers, Marine Frouin, et al.

### ► To cite this version:

Shannon A Mahan, Tammy M Rittenour, Michelle S Nelson, Nina Ataei, Nathan Brown, et al.. Guide for interpreting and reporting luminescence dating results. Geological Society of America Bulletin, 2022, 135 (5-6), pp.1480-1502. 10.1130/B36404.1 . hal-03820447v2

**HAL Id: hal-03820447**

**<https://hal.science/hal-03820447v2>**

Submitted on 17 Nov 2022

**HAL** is a multi-disciplinary open access archive for the deposit and dissemination of scientific research documents, whether they are published or not. The documents may come from teaching and research institutions in France or abroad, or from public or private research centers.

L'archive ouverte pluridisciplinaire **HAL**, est destinée au dépôt et à la diffusion de documents scientifiques de niveau recherche, publiés ou non, émanant des établissements d'enseignement et de recherche français ou étrangers, des laboratoires publics ou privés.



Distributed under a Creative Commons Attribution 4.0 International License

# Guide for interpreting and reporting luminescence dating results

**Shannon A. Mahan<sup>1,†</sup>, Tammy M. Rittenour<sup>2</sup>, Michelle S. Nelson<sup>2</sup>, Nina Ataee<sup>3</sup>, Nathan Brown<sup>4</sup>, Regina DeWitt<sup>5</sup>, Julie Durcan<sup>6</sup>, Mary Evans<sup>7</sup>, James Feathers<sup>8</sup>, Marine Frouin<sup>9</sup>, Guillaume Guérin<sup>10</sup>, Maryam Heydari<sup>11</sup>, Sebastien Huot<sup>12</sup>, Mayank Jain<sup>13</sup>, Amanda Keen-Zebert<sup>14</sup>, Bo Li<sup>15</sup>, Gloria I. López<sup>16</sup>, Christina Neudorf<sup>14</sup>, Naomi Porat<sup>17</sup>, Kathleen Rodrigues<sup>14</sup>, Andre Oliveira Sawakuchi<sup>18</sup>, Joel Q. G. Spencer<sup>19</sup>, and Kristina Thomsen<sup>13</sup>**

<sup>1</sup>U.S. Geological Survey Luminescence Geochronology Laboratory, Geosciences and Environmental Change Science Center, U.S. Geological Survey, Denver Federal Center, Denver, Colorado 80225, USA

<sup>2</sup>Department of Geosciences, Utah State University, 4505 Old Main Hill, Logan, Utah 84322, USA

<sup>3</sup>Department of Geography and Earth Sciences, Aberystwyth University, Aberystwyth SY23 3DB, Wales, UK

<sup>4</sup>Earth and Environmental Sciences, University of Texas, Arlington, P.O. Box 19049, Arlington, Texas 76019, USA

<sup>5</sup>Department of Physics, East Carolina University, 1000 E. 5th Street, Greenville, North Carolina 27858, USA

<sup>6</sup>School of Geography and the Environment, Oxford University Centre for the Environment, University of Oxford, Oxford OX1 3QY, UK

<sup>7</sup>School of Geography, Archaeology and Environmental Studies, University of the Witwatersrand, P.O. WITS 2050, South Africa

<sup>8</sup>Luminescence Dating Laboratory, University of Washington, Seattle, Washington 98195-3412, USA

<sup>9</sup>Department of Geosciences, Stony Brook University, 255 Earth and Space Science Building, Stony Brook, New York 11790, USA

<sup>10</sup>Univ Rennes, CNRS, Géosciences Rennes, UMR 6118, 35000 Rennes, France

<sup>11</sup>Institute of Earth and Environmental Sciences, University of Freiburg, Albertstrasse 23b, 79104 Freiburg im Breisgau, Germany

<sup>12</sup>Illinois State Geological Survey, Prairie Research Institute, University of Illinois at Urbana-Champaign, 615 East Peabody, Champaign, Illinois 6182, USA

<sup>13</sup>Department of Physics, Technical University of Denmark, DTU Risø Campus, Roskilde, Denmark

<sup>14</sup>Desert Research Institute, Division of Earth and Ecosystem Sciences, 2215 Raggio Parkway, Reno, Nevada 89512, USA

<sup>15</sup>Centre for Archaeological Science, University of Wollongong, Northfields Avenue, Wollongong NSW 2522, Australia

<sup>16</sup>Colombian Geological Survey, Nuclear Affairs Directorate, Luminescence Dating Laboratory, Diagonal 53 # 34-53, Bogotá 111321, Colombia

<sup>17</sup>The Geological Survey of Israel, Department of Geochemistry and Environmental Geology, 32 Yeshayahu Leibowitz Street, Jerusalem 9691200, Israel

<sup>18</sup>Luminescence and Gamma Spectrometry Laboratory (LEGaL), Institute of Geosciences, University of São Paulo, Rua do Lago, 562–Butantã, São Paulo, 05508-080, Brazil

<sup>19</sup>Department of Geology, Kansas State University, 108 Thompson Hall, Manhattan, Kansas 66506-3201, USA

## ABSTRACT

The development and application of luminescence dating and dosimetry techniques have grown exponentially in the last several decades. Luminescence methods provide age control for a broad range of geological and archaeological contexts and can characterize mineral and glass properties linked to geologic origin, Earth-surface processes, and past exposure to light, heat, and ionizing radiation. The applicable age range for luminescence methods spans the last 500,000 years or more, which covers the period of modern human evolution, and provides context for rates and magnitudes of geologi-


cal processes, hazards, and climate change. Given the growth in applications and publications of luminescence data, there is a need for unified, community-driven guidance regarding the publication and interpretation of luminescence results.

This paper presents a guide to the essential information necessary for publishing and archiving luminescence ages as well as supporting data that is transportable and expandable for different research objectives and publication outlets. We outline the information needed for the interpretation of luminescence data sets, including data associated with equivalent dose, dose rate, age models, and stratigraphic context. A brief review of the fundamentals of luminescence techniques and applications, including guidance on sample collection and insight into laboratory processing and analysis steps, is

presented to provide context for publishing and data archiving.

## INTRODUCTION

Geochronology is an essential tool for geoscience research. Results provide dates of deposits, minerals, and events and are used to calculate rates of Earth processes, climate and environmental change, cultural records, and the evolution of life. A recent vision statement by the U.S. National Academies of Sciences, Engineering, and Medicine (NASEM, 2020) highlighted the significant role of geochronology in Earth-science research. This report, appropriately entitled “Earth in Time,” outlines recommendations for U.S. National Science Foundation (NSF) funding and addresses points made in the “It’s About Time” (Harrison et al., 2015) community assessment of science priority questions. These

Shannon A. Mahan  <https://orcid.org/0000-0001-5214-7774>

<sup>†</sup>smahan@usgs.gov.

community-driven reports emphasize the need for increased access to geochronology through financial support of research, enhancement of laboratory facilities, development of cyber-infrastructure for data storage and sharing, as well as the retention of staff through training and career development.

Luminescence dating techniques include a versatile group of methods that provide age control for a broad range of geological and archaeological contexts (Fig. 1) (e.g., Lian and Roberts, 2006; Preusser et al., 2008; Singhvi and Porat, 2008; Rhodes, 2011; Liritzis et al., 2013; Aitken and Valladas, 2014; Brown, 2020). Luminescence signals can also be used to characterize mineral properties, geologic origin of minerals, and their past exposure to light, heat, and ionizing radiation (e.g., Sawakuchi et al., 2011; Guralnik et al., 2013; Gray et al., 2019). The applicable age range for standard luminescence methods spans the last 250,000 years (Murray and Olley, 2002; Rittenour, 2008; Rhodes, 2011; Murray et al., 2021). However, this age range

can be extended beyond half a million years or more in some situations (Yoshida et al., 2000; Watanuki et al., 2005; Ellerton et al., 2020) or by using specialized techniques (Buylaert et al., 2012; Ankjærgaard et al., 2013; Neudorf et al., 2019a; Kumar et al., 2021). This is an important window of geologic time as it covers part of the period of human evolution, provides context for rates and magnitudes of geological processes, and highlights societal needs linked to hazards, food, and water resources (Rittenour, 2008; Murray et al., 2021). For selected depositional settings and sample characteristics, minimum ages in the range of the last couple of decades to centuries can also be recovered (Madsen and Murray, 2009; Reimann et al., 2011; Spencer et al., 2019) with applications to forensic sciences (Larsson et al., 2005) and modern human impact on the global environment (Murray et al., 2021). Moreover, the broad age range of luminescence dating provides temporal resolution for paleoclimate records used in climate models, which allows a greater understanding of past

climate dynamics and prediction of future climate change (IPCC, 2019).

Luminescence technologies and instrumentation have advanced considerably in the past 20 years since the introduction of the modern single aliquot methodology (Murray and Roberts, 1998; Murray and Wintle, 2000). Growth in this field is evidenced by the recent rapid increase in the number of publications and instruments installed in laboratories (Fig. 2). The annual data output for each laboratory is restricted to 50–75 samples per instrument (with most laboratories having 1–4 instruments) due to time-intensive procedures needed to replicate burial doses. However, when combined in aggregate, the data generated from all luminescence laboratories exceed thousands of ages and publications produced each year. Given the improvement in luminescence dating technology, its growth in application and demand, and cross-disciplinary applications, researchers who use this technique need a clear outline of what information is needed for the publication and documentation of luminescence results.

Luminescence ages are reported in a variety of geoscience, archaeology, and physics journals, each with their own data reporting standards. Standardization in reporting requirements will help authors, reviewers, editors, and readers assess the nuances of the luminescence data and better compare results between publications and laboratories. Additionally, standardization has the potential to save time in the review process if minimum data requirements are included during manuscript submission. Finally, this standardization will help streamline reports from individual laboratories, facilitate the development of centralized data storage, and allow for a consistent curation and management system for the archival of luminescence data and ages, which is a requirement of many funding agencies.

The goals of this community-driven guide are to advise scientists, journal editors, reviewers, and readers on the most important aspects of luminescence data acquisition for the comprehensive interpretation and summarized reporting of results. While the age of the sample is a key piece of information, data related to the equivalent dose of radiation received following the event of interest (abbreviated  $D_E$ ), environmental dose rate ( $D_R$ , radioactivity of the sample and surroundings), and luminescence properties should also be published so that the age can be evaluated in greater context. This is particularly important given the rapidly advancing nature of luminescence dating techniques and methodology. While the focus of this paper is a community-led consensus and recommendation for publication

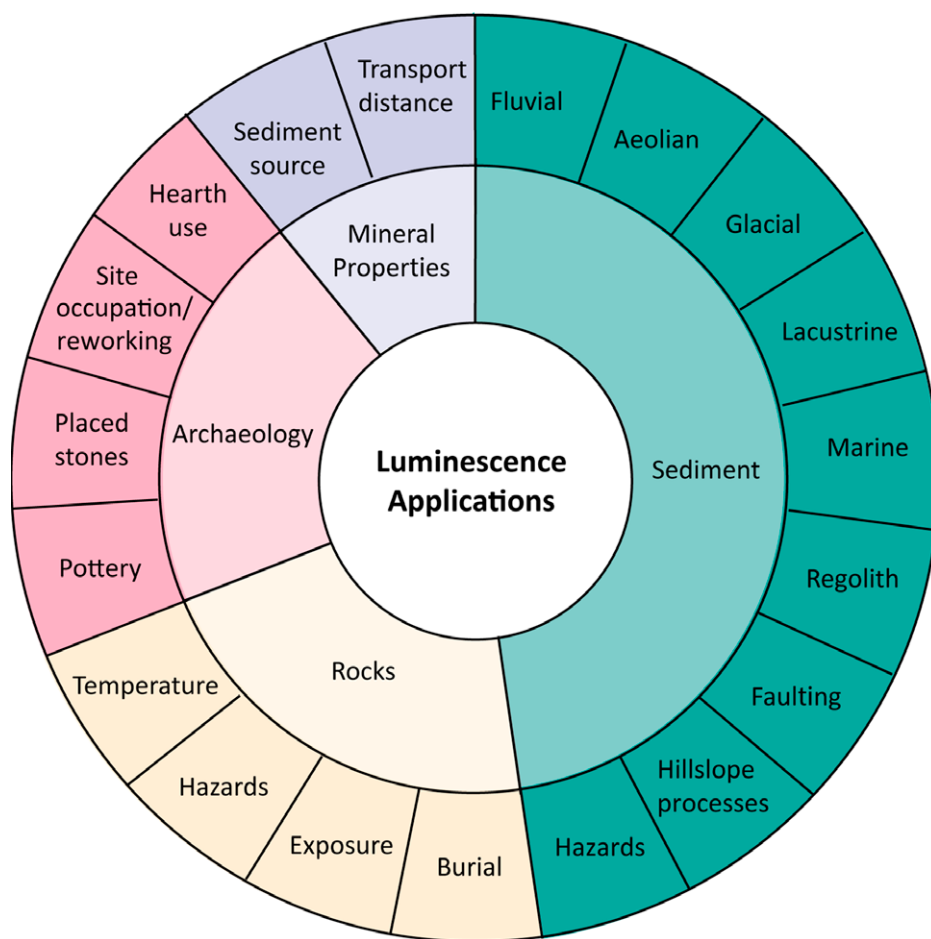


**Figure 1.** At-a-glance representation shows luminescence dating applications for minerals, rock, and sediment in the scientific fields of geology, archaeology, and mineral physics.

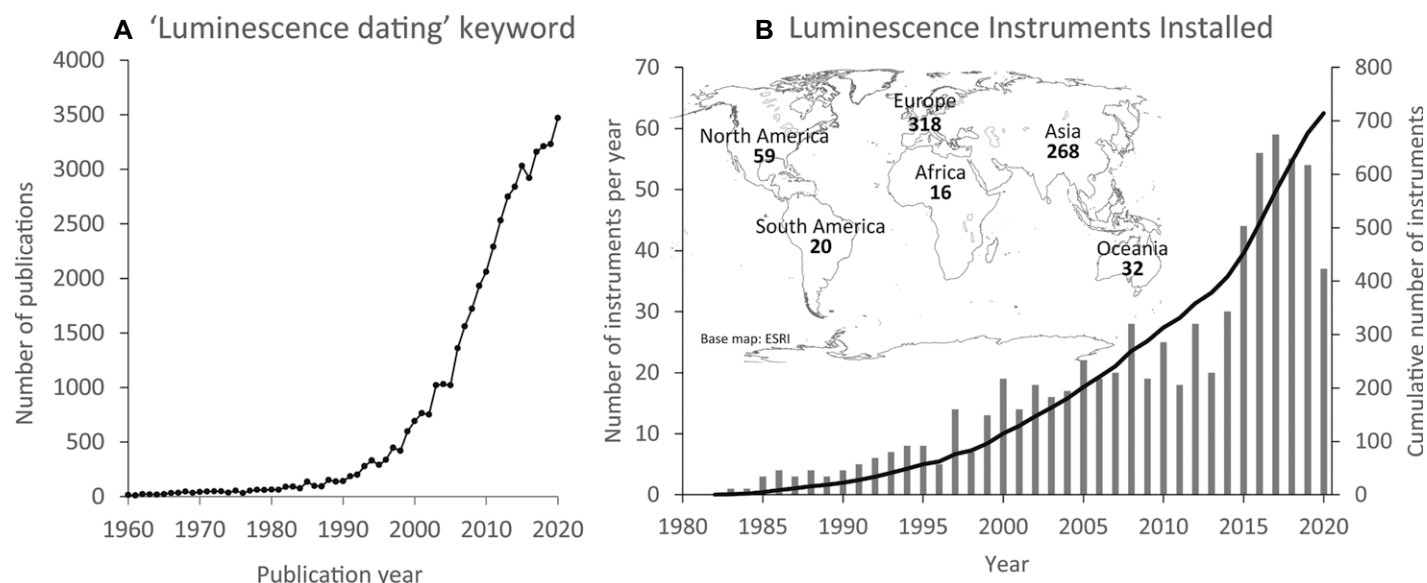


**Figure 2. (A) Graph shows publications and citations per year with “luminescence dating” as a keyword reported by Google Scholar for the years 1960–2020 CE. (B) Examples of growth in the field of luminescence geochronology: number of luminescence instruments installed in laboratories each year (data are from DTU Physics, Denmark, and Freiberg Instruments, Germany). Inset map displays the number of instruments per continent, which includes >200 laboratories across the globe.**

and reporting standards, we will also briefly discuss the fundamentals of luminescence techniques, provide a summary of commonly

used applications and data analysis methods employed in the field, and conclude with a path forward for managing luminescence data

resources. A list of terms and abbreviations used here and elsewhere in the literature is provided in Table 1.

**TABLE 1. LIST OF COMMON ABBREVIATIONS AND LUMINESCENCE TERMINOLOGY**

Term	Definition
Aliquot	Subsample of grains: 1 grain (single-grain aliquot or single-grain dating), 10 to hundreds of grains (small aliquot), 100 to thousands of grains (large aliquot).
Coarse-grain dating	Uses purified quartz or feldspar fine- to medium-sized sand grains, 60–250 $\mu\text{m}$ in diameter. Nonetheless, the most used grain size usually ranges between 90 $\mu\text{m}$ and 180 $\mu\text{m}$ .
$D_E$	Equivalent dose, laboratory radiation dose required to produce a luminescence signal that is equivalent to the natural dose of radiation the target mineral acquired since last exposure to heat or light, in Grays (Gy), where 1 Gy = 1 Joule/kg.
Disequilibrium	Due to loss or addition of radioisotope products of the U and Th decay-series chain, leads to disproportion between daughter and parent isotope.
$D_R$ , $\dot{D}$	Dose rate, rate of exposure to alpha ( $\alpha$ ), beta ( $\beta$ ), and gamma ( $\gamma$ ) radiation from radioisotopes of K, U, Th, Rb, and incoming cosmic rays in Gray (Gy) per kiloyears (Gy/kyr), (1 Gy = 1 Joule/kg). Average burial depth of the sample is required for cosmogenic dose-rate calculation. DRAC: Online Dose-Rate Calculator by Durcan et al. (2015).
$D_0$	Characteristic dose of saturation, where relationship between dose and resultant luminescence becomes non-linear. Saturation limit marks the maximum age attainable, typically $2^*D_0$ .
Fading	Athermal loss of luminescence signal in feldspar; correction is required for final age estimate.
Fine-grain dating	Uses polymineral (quartz and feldspar) small-aliquot silt grains, 4–11 $\mu\text{m}$ in diameter.
IRSL	Infrared-stimulated luminescence used for dating feldspars.
Luminescence age	Time since the last exposure of a sample to light or high heat. Calculated by dividing the $D_E$ (Gy) by the $D_R$ (Gy/kyr). Expressed in a (annum), ka, Ma, Ga. Datum is the date of sample collection, not yr B.P. (used only for radiocarbon dating).
Luminescence	Following eviction from a mineral lattice defect (trap), it is the signal generated by the release of a photon after an electron recombines in a lower energy state. The intensity is directly proportional to the number of trapped electrons, burial duration, and $D_R$ .
LM-OSL	Linear modulated (LM) OSL.
OSL	Optically stimulated luminescence (blue or green stimulation), used for dating quartz.
Multi-Grain dating	Multiple purified grains are measured using small or large aliquots. Individual $D_E$ values are obtained per aliquot. Commonly performed on very fine- to medium-sized sand grains, 60–250 $\mu\text{m}$ in diameter.
Overdispersion ( $OD$ , $\sigma$ )	Spread in $D_E$ values beyond analytical uncertainties. Causes include: partial bleaching, microdosimetry, intrinsic sensitivity, and/or post-depositional mixing.
Partial bleaching	Incomplete resetting of a prior luminescence signal due to insufficient duration and intensity of sunlight or heat exposure.
Post-IR IRSL	Infrared stimulated luminescence (IRSL) of feldspar at an elevated temperature following infrared (IR) stimulation.
Post-depositional mixing	Stratigraphic displacement of grains in a sedimentary column through disturbance following deposition (e.g., soil processes, bioturbation, and cryoturbation).
Sensitivity	Luminescence intensity per unit mass per unit radiation dose, which is often related to the source geology and sediment history.
Single-aliquot dating	Methods where an individual $D_E$ value is calculated for each aliquot measured.
SAR	Single-aliquot regenerative dose method, developed by Murray and Wintle (2000).
Single-grain dating	Laser is used to stimulate one grain at a time to calculate an individual $D_E$ value per grain. Commonly performed on fine-grained sand, 150–250 $\mu\text{m}$ in diameter.
Statistical models	Used to calculate representative $D_E$ value(s) from a well-bleached, partially bleached, or multi-modal population of individual single-grain or small-aliquot $D_E$ values. Common models include minimum age model, common age model, central age model, finite mixture model (Galbraith and Roberts, 2012), and average dose model (Guérin et al., 2017). Graphical representations of data and models: Radial plot, abanico plot, kernel density plot, histogram, and probability density function.
Thermochronology	Recent advancement in luminescence methods used to constrain low-temperature cooling rates of bedrock.
TL	Thermoluminescence, dating method that uses heat as a stimulation source to release electrons from traps.

TABLE 2. MINIMUM REPORTING CRITERIA FOR LUMINESCENCE AGES

Primary Reporting Criteria	Supplemental Information
<ul style="list-style-type: none"> <li>• Sample ID, lab identification number</li> <li>• Luminescence signal measured (optically stimulated luminescence, infrared stimulated luminescence, thermoluminescence, etc.)</li> <li>• Mineral and grain-size analyzed</li> <li>• Equivalent dose (<math>D_E</math>) and uncertainty</li> <li>• Dose rate (<math>D_R</math>) and uncertainty</li> <li>• Age and uncertainty</li> <li>• Method of <math>D_E</math> determination (e.g., single-aliquot regenerative dose)</li> <li>• Method of <math>D_R</math> determination (e.g., neutron activation analysis, inductively coupled plasma–mass spectrometry, gamma spectrometry, <math>D_R</math> calculator used)</li> <li>• Aliquot size (single-grain or multi-grain)</li> <li>• Number of aliquots analyzed</li> <li>• Statistical model used for <math>D_E</math> calculation</li> <li>• Year of sample collection (datum for age)</li> <li>• Radionuclide concentrations or activity and water content used to calculate <math>D_R</math></li> <li>• Sample burial depth, elevation, and geographic coordinates used for cosmic dose-rate calculation</li> </ul>	<ul style="list-style-type: none"> <li>• Instrumental parameters (e.g., reader type, year, light-emitting diode output, filter types)</li> <li>• Measurement parameters (e.g., preheat temperature, stimulation wavelength and intensity, detection wavelength)</li> <li>• <math>D_E</math> distribution plots, overdispersion</li> <li>• Example dose-response and signal-decay curves</li> <li>• Parameters related to luminescence signals (e.g., fast component, linear modulated–optically stimulated luminescence and thermoluminescence glow curves)</li> <li>• Fading rate and calculation method (for feldspar)</li> <li>• Data quality checks (e.g., dose recovery tests, aliquot rejection criteria)</li> <li>• <math>D_R</math> components (<math>\alpha</math>, <math>\beta</math>, and <math>\gamma</math>), internal dose rate, alpha efficiency (<math>\alpha</math>-values) where relevant</li> </ul>

*Notes:* Primary criteria should be included in the main text of the publication, while secondary criteria can be reported in the supplemental material.

## PUBLICATION GUIDELINES

In time, all hard won, state-of-the-art data will become legacy data if not adequately reported and archived. It is the goal of this paper to set a community-led standard for luminescence data reporting such that this information remains useful well into the future, long after the laboratory personnel and researchers have retired, and methodologies have advanced. Moreover, geochronology data published without metadata are not as valuable because they lack the context required by interdisciplinary research and regional to global-scale modeling. The first step toward building geochronology data resources is to have a minimum number of attributes necessary to interpret the age of a luminescence sample from a third-party point of view. Inclusion of nuances involved with luminescence dating are meaningful now and in ways yet to be explored. We present recommendations for luminescence age reporting based on commonly accepted reporting requirements and previous recommendations (Duller, 2008a; Preusser et al., 2008; Nelson et al., 2015; Lancaster et al., 2016; Ancient TL, 2017; Bateman, 2019). Table 2 presents basic guidelines for authors and journal editors regarding informa-

tion to be reported in publications. Examples of reporting tables for the  $D_E$  (lab-based dose of radiation needed to replicate the natural luminescence signal) and the  $D_R$  (rate of environmental radiation exposure) are provided in Table 3.

The resultant luminescence ages, as well as their related  $D_R$  and  $D_E$  information, should be included in publications, documents, and reports. Other critical information includes the mineral and luminescence signal measured; the size of the aliquots used for  $D_E$  measurements; the statistical model used to analyze the  $D_E$  data; geographic location, sample depth, and water content; and the method of radionuclides determination (for  $D_R$  calculation).

Publications with detailed and informative supplemental sections provide a variety of data that support the luminescence age results. Details related to specific luminescence properties and data can be placed in the main text but are often better suited for a supplemental material section. These details may include  $D_E$  distribution plots (e.g., radial, abanico, or kernel density plots), relative standard deviation and overdispersion within the data (abbreviated as OD or  $\sigma$ , a measure of spread or scatter in the  $D_E$  distribution; Galbraith et al., 1999), and quality

assessment criteria used to support the inclusion of  $D_E$  data in age calculation (e.g., López et al., 2018). Supplemental materials may also include information about the measurement protocol, such as stimulation and detection wavelengths, preheat temperatures, and other parameters used for  $D_E$  measurement. Other information in supplemental data sections could also include sample response to replication and data quality tests (e.g., dose-recovery and preheat-plateau tests), the influence of variable water content and dose-rate disequilibrium, sampling site profiles, and photographs (e.g., Feathers et al., 2020; Pazzaglia et al., 2021; Tecsá et al., 2020). Ideally, well-documented and researched papers will also include signal decay curves (for optically stimulated luminescence [OSL]) or glow-curves (for thermoluminescence [TL]), representative dose response curves, information on the luminescence signal properties (characteristic dose of saturation, proportion of fast-decay component, etc.), and tests for dose-rate disequilibrium.

## ANALYSIS TIMELINE AND WORKFLOW

The workflow for luminescence dating methods generally follows that of other geochronological techniques with steps for field collection, laboratory processing and measurement, data analysis, publishing, and data archiving. The timeline for laboratory analysis is an exception to other geochronological techniques in that the luminescence measurements can be lengthy, on the order of a week to multiple months for each sample batch (Fig. 3). This is related to the dose of interest, number of available instruments and personnel in the laboratory, storage times for various measurements, potency of the radiation source on the instrument, and replicated measurement requirements. Generally, older samples take longer to measure due to the time needed to build dose response curves encompassing the  $D_E$  and burial doses. All samples require tens to thousands of replicate analyses, on multi-grain or single grain aliquots of sand, respectively, to generate each individual age determination. Additional time is required for

TABLE 3. EXAMPLE TABLE FOR REPORTING LUMINESCENCE AGES AND DOSE-RATE INFORMATION

Sample/ laboratory number	Depth (m)	H <sub>2</sub> O (wt%)	K (%) <sup>*</sup>	Th (ppm) <sup>*</sup>	U (ppm) <sup>*</sup>	Cosmic dose rate (Gy/kyr) <sup>†</sup>	Total dose rate (Gy/kyr) <sup>§</sup>	Number of aliquots <sup>#</sup>	$D_E$ (Gy) <sup>**</sup>	OSL age $\pm 1\sigma$ (ka) <sup>††</sup>
Unique ID	0.5	4.0	1.44 $\pm$ 0.04	3.1 $\pm$ 0.3	0.8 $\pm$ 0.1	0.15 $\pm$ 0.02	1.90 $\pm$ 0.10	24 (30)	7.41 $\pm$ 0.99	3.89 $\pm$ 0.27

<sup>\*</sup>Radioelemental determination conducted using inductively coupled plasma–mass spectrometry and inductively coupled plasma–optical emission spectrometry techniques.

<sup>†</sup>Cosmic dose rate calculated following Prescott and Hutton (1994).

<sup>§</sup>Dose rate calculated using the Dose Rate and Age online calculator (Durcan et al., 2015).

<sup>#</sup>Number of aliquots used in age calculation and number of aliquots analyzed in parentheses.

<sup>\*\*</sup>Equivalent dose ( $D_E$ ) calculated using the central age model with 1 standard error (se) uncertainty (Galbraith and Roberts, 2012).

<sup>††</sup>Age analysis using the single-aliquot regenerative-dose procedure of Murray and Wintle (2000) on 2 mm small aliquots of 90–150  $\mu$ m quartz sand. OSL—Optically stimulated luminescence.



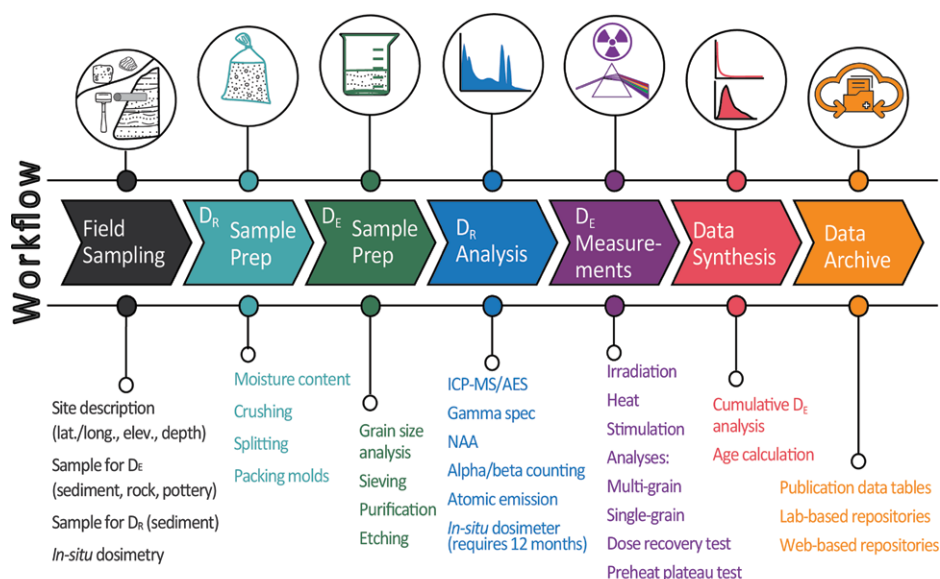


**Figure 3. Generalized workflow for laboratory processing of luminescence samples following field collection and submission to a luminescence laboratory is shown. Preparation and analyses of dose rate ( $D_R$ ) and equivalent dose ( $D_E$ ) samples are often done simultaneously. Individual  $D_E$  measurements constitute most of the analytical time required. ICP-MS/AES—inductively coupled plasma–mass spectrometry/atomic emission spectrometry; NAA—neutron activation analysis.**

fading measurements of feldspar samples (loss of signal with time).

Figure 3 illustrates the common workflow stages for luminescence dating analysis. Due to the length of time required in the laboratory and the demand for the dating method, it is rare to receive results back in less than six months. Consequently, patience and proper planning is essential to meet project deadlines. It is highly recommended and often required by the laboratory that proposed field-sampling methods, target sample materials, and locations are discussed with a luminescence specialist prior to sampling.

Depending on the scope of the project, number of samples, and location of field sites, field sampling can be completed within a couple of days following reconnaissance, although it may also span multiple weeks for larger projects in complex or difficult-to-access regions. Descriptions of the target material and the geologic, geomorphic, and archaeological context are needed for each sample. These on-site descriptions and assessments are expected to take the bulk of the time in the field as the actual sampling can be completed relatively quickly (<1 h per sample). As with many dating techniques, the interpretations and accuracy of luminescence results are directly linked to the characteristics of the target material, the depositional and post-depositional context, and methods of field collection completed prior to laboratory analysis.

## PRINCIPLES AND ASSUMPTIONS OF LUMINESCENCE DATING

Luminescence dating methods provide an age estimate of the last exposure of minerals (typically quartz or feldspar) to light or heat, which

resets the luminescence clock (Aitken et al., 1964; Huntley et al., 1985). Following burial and removal from heat, exposure to ionizing radiation from radioisotopes from within the sample and the surrounding environment and incident cosmic radiation leads to the accumulation of trapped charge (ionized and missing electrons) within defects in the crystal-lattice structure (Fig. 4). Part of this stored energy is released as luminescence (photons of light) when prepared mineral separates are exposed to controlled light or heat conditions in the laboratory. The intensity of luminescence released by a sample is related to the amount of radiation absorbed over time (following a saturating exponential function) and is related to the radioactivity of the sample site. In the laboratory, the naturally acquired luminescence signal (the natural signal) is compared to luminescence generated by laboratory irradiation to calculate the accumulated radiation exposure the sample received in nature. The radiation dose required to reproduce the natural luminescence signal is known as the  $D_E$  (equivalent dose) and is measured in Grays (Gy, where 1 Gy = 1 Joule/kg). The environmental radioactivity of the sample site is known as the  $D_R$  (dose rate), reported in Gy/kyr (or mGy/yr), and includes ionizing radiation from alpha, beta, and gamma ( $\alpha$ ,  $\beta$ , and  $\gamma$ ) decay of radioisotopes of U and Th decay-series chain and K, plus incident cosmic radiation. The time since last exposure to light or heat (age) is calculated by dividing the  $D_E$  by the  $D_R$  (Equation 1). Ages are reported in calendar years, and the datum is the year of sample collection. Fol-

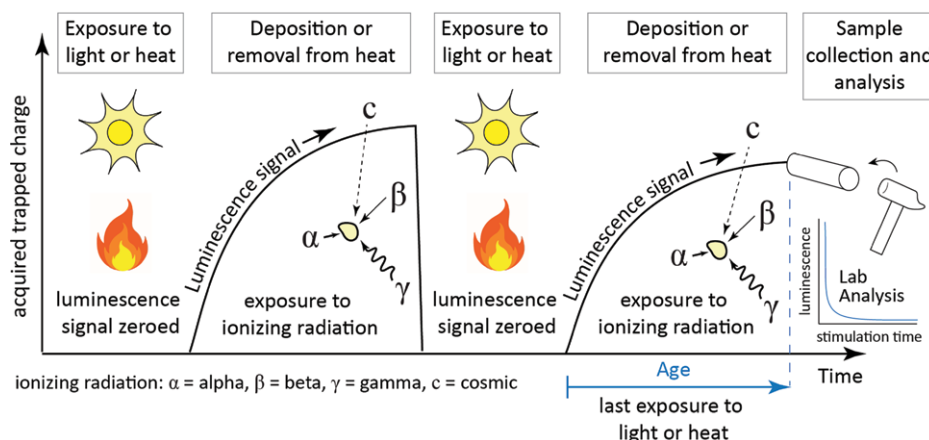


**Figure 4. Illustration depicts the concepts behind luminescence dating techniques, and two exposure and burial events are shown. In sequence, the sample is exposed to light or heat, and any previous luminescence signal is reset (zeroed). Sediment deposition and burial allow for the build-up of a trapped charge population because of exposure to ionizing radiation from the surrounding environment and existing cosmic radiation. The optically stimulated luminescence (OSL) sample is collected following another exposure and burial cycle. The luminescence signal measured in the laboratory is related to the time since last exposure to light or heat and the environmental radioactivity at the sample site.**

lowing SI convention, ages should be reported in units of a (annum), ka, Ma, or Ga (thousands, millions, and billions of years ago), while durations of time are references as yr, kyr, Myr, and Gyr (Aubry et al., 2009). Luminescence ages should never be reported in yr B.P. (1950 CE), the datum exclusively reserved for radiocarbon dating due to bomb testing (Broecker and Walton, 1959; Heaton et al., 2020).

$$\text{Age} = \frac{\text{Equivalent Dose (Gy)}}{\text{Dose Rate} \left( \frac{\text{Gy}}{\text{kyr}} \right)} \quad (1)$$

## Assumptions

One of the main assumptions with luminescence dating is related to whether the luminescence signals in the targeted mineral grains were completely reset prior to the event of interest. For applications related to dating sedimentary deposits, this resetting (bleaching) needs to have occurred during sediment transport (Duller et al., 2000; Brown, 2020; and Gray et al., 2020). Incomplete zeroing of the luminescence signal (partial bleaching) will produce a residual latent dose that the subsequent burial dose will be added onto, which leads to overestimates of age. Another important assumption regarding the geologically acquired dose ( $D_E$ ) is that sediments of different light and radiation exposure histories have not been mixed following deposition. Bioturbation from plant roots and animal burrows, pedoturbation from shrink-swell processes and soil formation (i.e., clay translocation and mineral precipitation), cryoturbation from ice growth and melting, and anthropogenic disturbance can mix sediment vertically and horizontally, making it difficult to estimate  $D_E$  from a broadly dispersed and mixed population (Fuchs and Lang, 2009; Gray et al., 2020). In the case of determining the manufacturing date of pottery or fire-exposed rock, it is assumed that the sample has not been re-exposed to fire (e.g., Ideker et al., 2017; Roos et al., 2020). With all methods, it is also assumed that the mineral grains do not lose trapped charge over burial time. Feldspars, which are known to be affected by anomalous fading (loss of signal over time), carry the assumption that the rate and severity of the fading can be accurately estimated, and corrected for in the laboratory, or otherwise circumvented using techniques that sample more stable traps (Thomsen et al., 2008).

Assumptions regarding the environmental  $D_R$  are linked to constant radioactivity over time. For example, it is assumed that there are little to no additions or losses in radioelements, secular equilibrium has been maintained between par-

ent and daughter nuclides of the uranium and thorium series (production rate equals decay rate), and that the time-averaged moisture content is known or can be estimated. Finally, it is assumed that the sampling was done correctly, the  $D_E$  sample was not exposed to light, and the  $D_R$  sample (or in situ measurement) is representative of the surrounding ionizing radiation reaching the sampled minerals.

## Considerations

Important questions, when considering the choice of a geochronological method for a research project, are linked to the applicable age range of the method and the type of material needed for analysis. As described above, luminescence techniques provide an age estimate of the last time minerals within sediment, rock, or pottery were exposed to light or heat, which resets the luminescence signal. Considerations for sample selection and methods include: the mineral content and grain size of the sample, the age of the event to be dated, the likelihood that the luminescence signal was reset at the time of the event of interest and not subsequently disturbed, environmental radioactivity surrounding the sample, and the luminescence characteristics of the target mineral. These factors all play a role in the suitability of sample settings and target materials and affect the ability to obtain accurate luminescence results. Factors related to limits of application and age range are discussed below.

## Grain Size and Mineral Content

Typical minerals with well-characterized luminescence properties and methods developed for luminescence dating are quartz and potassium (K) feldspar, although other minerals and biogenic materials have been explored (e.g., Duller et al., 2009; Mahan and Kay, 2012). Key to successful application of luminescence dating is not only the presence of these target minerals, but also their abundance and grain size. Due to constraints largely related to dose-rate calculations, applicable grain sizes are either in the very fine to fine sand (63–250  $\mu\text{m}$ ), coarse silt (30–63  $\mu\text{m}$ ), or very fine silt (4–11  $\mu\text{m}$ ) fractions. These grain-size ranges allow for the accurate calculation of beta-dose attenuation and the removal or full incorporation of alpha doses based on grain size and etching of the outer rims of grains (Aitken, 1985; Guérin et al., 2012; Martin et al., 2014). Sample grain-size, mineral content, and volume characteristics need to be enough to ideally allow at least 1–2 g of purified mineral separates of a narrow grain-size range (typically within the 100  $\mu\text{m}$  range for sand),

although results can be obtained from less sample in some cases. Coarse-grain dating of very fine- to fine-grained sand is preferred over fine-grained dating of silt due to the ability to purify samples into a single mineral composition. Fine-grained dating typically uses polymineral separates, which leads to challenges arising from the contribution of different luminescence signals from multiple minerals, although fine-grained dating may be preferable in complex dose-rate environments due to less reliance on the gamma dose rate.

## Maximum Age Range

The applicable age range for luminescence dating is sample specific and based on combined variables related to luminescence properties and  $D_R$  environments. Luminescence dating does not have the precise minimum and maximum age limits typical of other radiometric dating techniques defined by half-life decay rates. The maximum age for a luminescence sample is controlled by the level of radiation exposure at which saturation is reached, the environmental dose rate, as well as the general stability of the signal used for dating.

In the laboratory, the luminescence response to a range of radiation doses is recorded, and the resulting dose response curve is fitted with a suitable function (e.g., a saturation exponential). The  $D_E$  of a sample is then obtained by interpolation onto the dose response curve. In the low-dose region, the signal growth follows a linear function, but at a higher radiation dose there is a nonlinear increase in luminescence signal, and the dose response is best described by a saturating exponential. The characteristic dose of saturation ( $D_0$ ) of this dose response curve is the point where exposure to higher radiation does not produce a linear increase in luminescence signal; instead, the results are best fit with a saturating exponential beyond this point. Typical  $D_0$  levels of ~50–200 Gy for quartz (Roberts and Duller, 2004) and ~500 Gy for feldspar (Kars et al., 2008) have been reported using standard single-aliquot regenerative dose methods (SAR; Murray and Wintle, 2000). The maximum  $D_E$  value for a sample is recommended to be less than  $2 \cdot D_0$  (Wintle and Murray, 2006) due to asymmetry in the calculated  $D_E$  values above this point because of interpolation onto a saturating exponential dose response curve (e.g., Murray and Funder, 2003).

Environments with low environmental radioactivity will allow older ages to be captured prior to saturation of the luminescence signal. The maximum age for routine quartz luminescence dating is ca. 100–200 ka using standard methods, considering typical saturation levels

around 100–200 Gy and dose rates of 1–2 Gy/kyr. It is important to reiterate that dose response characteristics and saturation levels vary greatly between samples from different geological contexts (Mineli et al., 2021) and even grain-to-grain within the same sample (Yoshida et al., 2000). Reliable quartz ages matching independent chronometers have been obtained for samples as old as 500 ka and approaching 1 Ma using new techniques (Arnold et al., 2015; Fattahi and Stokes, 2000; Ankjærgaard et al., 2013) and in low dose environments (Ellerton et al., 2020). Luminescence dating of feldspar has the potential to extend the age range to >500 ka due to higher saturation levels (Buylaert et al., 2012) despite the higher dose rate than quartz.

### Minimum Age Range

Luminescence dating has been successful in dating recent and historic sediments from the last several decades and centuries (Madsen and Murray, 2009; Spencer et al., 2019). The minimum age is largely defined by the radioactive environment of the sample ( $D_R$ ), its luminescence sensitivity, and the efficiency at which previously acquired signals were reset at the time of last exposure to heat or light. Unlike the challenges of dating older deposits linked to saturation levels, high  $D_R$  environments (typically greater than ~2.5 Gy/kyr for quartz) are often important for acquiring a measurable signal (above background levels; depending on luminescence sensitivity) in historical and recent samples. In young deposits, the effects of partial bleaching, or incomplete zeroing of the luminescence signal, can lead to substantial residual doses and age overestimates (Olley et al., 1998). Only sediments most likely to have been exposed to sufficient light or heat prior to deposition should be collected when trying to resolve recent events (Jain et al., 2004). Use of single-grain dating can also help to identify the grains that were reset at the time of deposition (Duller, 2008b).

### Geologic Source and Luminescence Sensitivity

Experienced luminescence practitioners have learned that there are geological and geographical regions where some quartz and feldspar from rocks and sediments can have problematic luminescence behavior for dating purposes. While these regions are commonly of the greatest interest to geologists (tectonically active mountain belts, glacial environments, and formerly glaciated environments), they can provide some of the greatest challenges for luminescence dat-

ing. Publications documenting problems with luminescence signals and behavior from these regions are available but are commonly obscure to non-specialists due to complex methods of testing and the jargon used to describe the problems with luminescence from these areas (e.g., Berger et al., 2001; Lawson et al., 2012). Moreover, publishing research failures is less rewarding and such papers are less likely to be highlighted in high-impact journals, which further reduces publicity of these problem settings to non-specialists.

Luminescence sensitivity (signal brightness) of quartz varies considerably between geographical and geological regions, deposit type, and even between individual grains in the same sample (Fig. 5). In fact, most sediment grains do not produce a luminescence signal; typically, only 1%–5% of quartz grains (Duller, 2008b) contribute to the luminescence of a multi-grain aliquot. The luminescence sensitivity of quartz recently released from igneous or metamorphic rock is relatively low (Sawakuchi et al., 2011; Mineli et al., 2021) and is enhanced by repeated cycles of Earth-surface processes of sediment transport and exposure to light, heat, and radiation (Moska and Murray, 2006; Pietsch et al., 2008; Gray et al., 2019). Regions sourcing quartz grains with high-luminescence sensitivity, and therefore best suited for luminescence dating, usually have slow erosion rates, long transport distances, have been exposed to long-term sediment cycling (i.e., erosion-transport-deposition cycles), and are preferably sourced from sedimentary bedrock. Areas of active orogens with rapid bedrock erosion and volcanic activity, such as the Southern Alps of New Zealand (Berger et al., 2001; Preusser et al., 2006), California and the Mojave Desert (Lawson et al., 2012; McGregor and Onderdonk, 2021), the Andes (Steffen et al., 2009; del Río et al., 2019), Himalayas (Richards, 2000), and Alaska and the Yukon (Demuro et al., 2008) are a few locations that have been noted as containing quartz with low sensitivity and feldspar with high fading rates and thus require extra measures during age determination.

Methods involving isolation of the fast-decay signal in quartz used for dating (e.g., Bulur et al., 2000; Ballarín et al., 2007; Bailey, 2010; Cunningham and Wallinga, 2010; Durcan and Duller, 2011; Combès and Philippe, 2017) and infrared stimulated luminescence (IRSL) signals with lower (Thomsen et al., 2008; Buylaert et al., 2009) or negligible (Thiel et al., 2011; Li and Li, 2011; Lamothe et al., 2020) fading rates in feldspar have been developed, but tectonically active settings remain challenging to date. Feldspars may be dim and insensitive in volcanic regions when the sediments are dominated by Ca or Na

feldspars, which are often not removed in density separation because the grains contain intergrown minerals (Sontag-González et al., 2021). Researchers working in volcanic-sourced terrane and active orogens would be well served to discuss research objectives and sample-selection goals with luminescence laboratory personnel prior to project design, application for funding, and sample collection.

### Precision, Accuracy, and Sources of Uncertainty

Choosing the appropriate geochronological technique, with the precision and accuracy that matches the resolution needed to answer the research questions, is a common conundrum. Precision of a technique reflects the reproducibility of the method and is incorporated in the reported uncertainty of an age, while accuracy is related to how the results relate to the true age of a deposit or feature and can only be ascertained by multiple lines of evidence (or independent geochronometers) dating the same event.

Tests of the accuracy of all dating techniques are challenging due to the vagaries of geologic time and different materials and systems dated in each. Comparison of luminescence and radiocarbon ages from a deposit is commonly used to test the accuracy of the luminescence ages; however, radiocarbon provides an age estimate of the death of an organism, while the luminescence age of the surrounding sediment provides the timing of sediment exposure to light prior to deposition. These are two separate events, and it is expected that the organism pre-dates the deposit in most situations (Blong and Gillespie, 1978; Schiffer, 1986). An added uncertainty when comparing luminescence and radiocarbon ages comes from the need to calibrate radiocarbon ages and the broad, non-singular age ranges that commonly result (Telford et al., 2004). Nonetheless, the question of the accuracy of luminescence dating has been investigated and addressed in multiple studies, and it has been shown that reproducible ages are consistent with other age controls when applied to suitable settings (Murray and Olley, 2002; Rittenour, 2008; Madsen and Murray, 2009; Arnold et al., 2015).

Several sources of systematic and random uncertainty in  $D_E$  determinations related to the instrumentation, measurement protocols, bleaching history, and geologic setting. Poisson (counting) statistics are related to the instrumental detection sensitivities and the luminescence brightness (sensitivity) of the sample. Instrument-based sources of error can include temperature variation during heating, power instability of light stimulation, movement of discs within the instrument and loss of sediment between



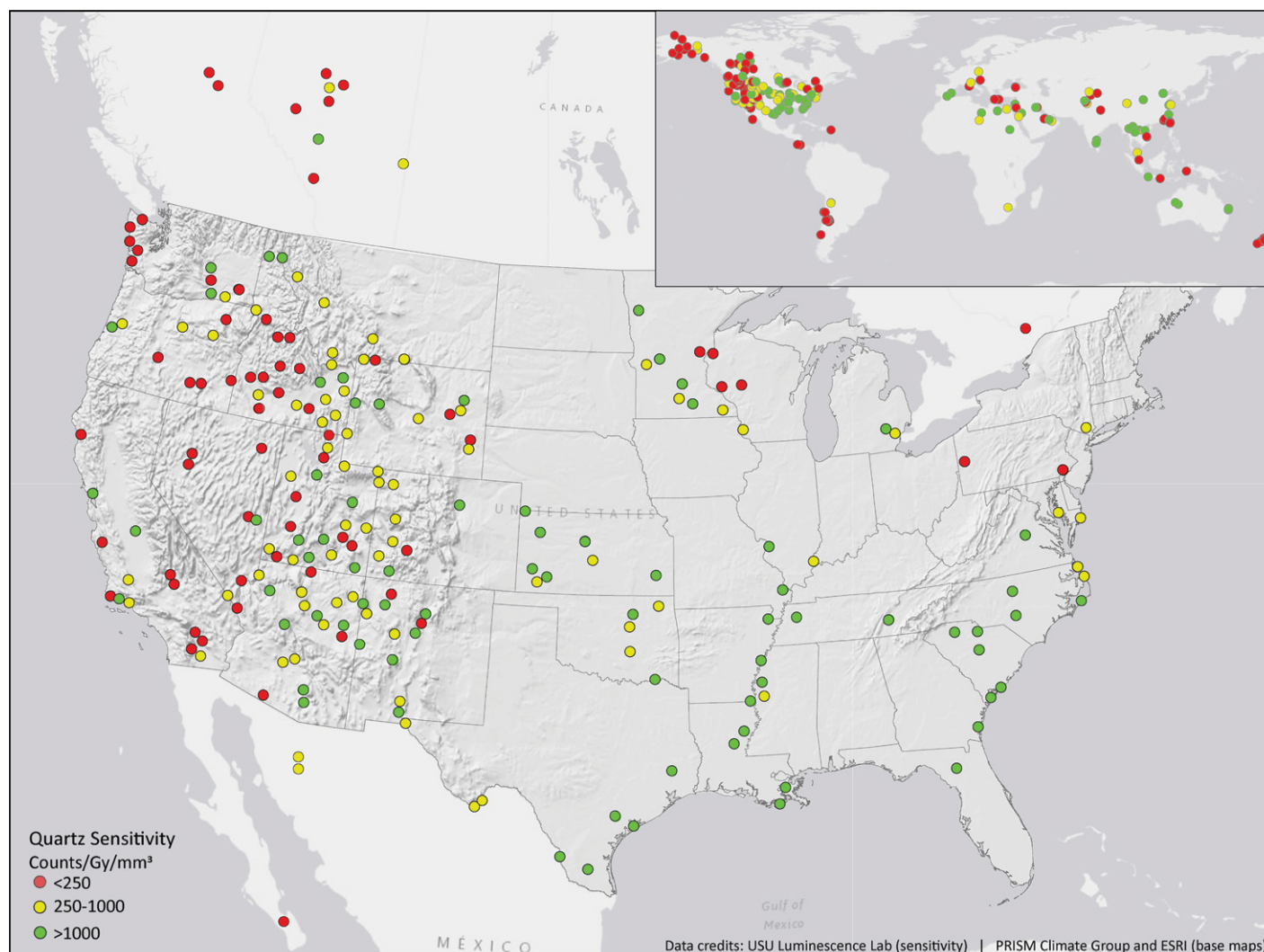


**Figure 5.** General map of quartz luminescence sensitivity displays the wide range of luminescence characteristics across physiographic and geologic regions. Samples incorporated in this map are not representative of all sediment sources and settings in a region and should not be used to determine the feasibility of future projects. All contributing data come from samples that produced viable luminescence ages. Data points represent luminescence sensitivity in signal per dose per volume. Red is relatively low-sensitivity quartz (below 250 counts/Gy/mm<sup>3</sup>), yellow is relatively moderate-sensitivity quartz (250–1000 counts/Gy/mm<sup>3</sup>) and green is relatively high-sensitivity quartz (>1000 counts/Gy/mm<sup>3</sup>).

successive measurements, and repositioning of the laser for single-grain measurements, etc.

Uncertainty in  $D_E$  measurement is also related to the performance of measurement protocols. Sources of error include imperfect correction of sensitivity changes across measurement cycles and different radiation conditions between the laboratory and nature, such as the rate of irradiation (laboratory dose rates are delivered at a rate  $\sim 10^8$ – $10^9$  greater than natural rates). Other uncertainties may also arise if the measured signals have unwanted physical properties, such as thermal instability (Sontag-González et al, 2021; Liu et al., 2019) and fading (Wintle, 1973).

Uncertainty associated with  $D_R$  calculation is typically  $\pm 5\%$ – $10\%$  and includes random and systematic error related to instrumentation and environmental conditions. Uncertainties include assumptions of secular equilibrium in the U and Th decay chain that cause changing  $D_R$  over time due to additions and losses of daughter products (Olley et al., 1996). The conversion factors used to calculate  $D_R$  from radionuclide concentrations (Guérin et al., 2012), the degree of beta and alpha attenuation due to grain size (Wallinga and Cunningham, 2015), and the level of internal radioactivity of grains, particularly with feldspars, are important considerations. Uncertainties in cosmic and gamma

$D_R$  due to changes in burial depth, and variations in incident radiation (Prescott and Hutton, 1994), are typically assumed to be 10%. Uncertainties in the cosmic  $D_R$  are greater in settings with heterogeneous shielding, temporal changes in sediment overburden, or low-dose environments, where the cosmic dose may contribute up to 50% of the  $D_R$  (Rink and López, 2010), but the contribution from cosmic dose is typically less than 10% of the total dose rate for most samples. One of the greatest sources of  $D_R$  uncertainty is linked to the estimation of water content during burial. Interstitial water content significantly attenuates radiation such that a 10% change in water content results in

a ~10% change in  $D_R$  and thus in the resulting age estimate (Aitken, 1998).

Luminescence ages are commonly reported at one sigma standard error (denoted as  $1\sigma$  or  $1\text{ se}$ ) and include both random (sample specific) and systematic (instrument and method-based) errors. Random error from scatter in  $D_E$  measurements commonly makes up the largest portion of this uncertainty. Reported uncertainties typically range from 5%–15% of the age (relative standard error, RSE) but can be as large as >50% RSE in samples with high  $D_E$  overdispersion (scatter beyond instrumental error) due to partial bleaching, post-depositional mixing, and grain-to-grain scatter from microdosimetry (e.g., Duller, 2008b). Assessment of all sources of uncertainty incorporated with instrument calibration and  $D_R$  calculation indicates that the maximum precision obtainable is ~5% RSE (Murray and Olley, 2002; Guérin et al., 2013). Given that luminescence errors are reported in relation to the age, a 5% RSE reflects a reported error range of 5–5000 years for samples 100–100,000 years in age, respectively.

## SAMPLE COLLECTION

The suitability of geological or archaeological materials for luminescence dating depends upon the ability to precisely and accurately determine the two components of the age equation: the acquired  $D_E$  and the environmental  $D_R$ . Important considerations for sample selection that are related to the  $D_E$  include: (1) characteristic saturation dose ( $D_0$ ) and sensitivity (luminescence intensity per unit mass per unit dose) particularly for old and young deposits, respectively (Wintle and Murray, 2006); (2) likelihood of signal resetting prior to the event of interest (e.g., sediment deposition), an issue that is important when dealing with young samples (Jain et al., 2004), and (3) likelihood of post-depositional processes such as mixing (bioturbation) (Bateman et al., 2003), weathering, pedogenesis, and diagenesis that can affect  $D_E$  scatter and  $D_R$  changes over time.

When designing research projects and selecting sample sites, it is important to consider the target event of interest and what the luminescence results represent. Figure 1 shows an array of applications in which luminescence dating is commonly used. Sample sites and materials collected for dating should be carefully selected to avoid sampling units with high deposition rate and/or sediment disturbance, which can lead to partial bleaching and mixed-age  $D_E$  distributions due to post-depositional mixing from bioturbation (Cunningham et al., 2015; Smedley and Skirrow, 2020). Exceptions include projects where the purpose is to date high-flow events

such as floods or tsunami events (Reinhardt et al., 2006; López et al., 2018; Riedesel et al., 2018; Liu et al., 2020) or paleosols (Feathers et al., 2020; Groza-Săcaci et al., 2020) or to understand processes of archaeological site formation (Frouin et al., 2017a; Araújo et al., 2020). It is critical in these situations that the luminescence specialist understands the complete context of the site and rationale for sample collection and the target event, preferably by being on-site during collection.

Ideal conditions for  $D_R$  environments surrounding a sample are those that are homogeneous with regard to the spatial distribution of radioelements of U, Th, and K (Guérin et al., 2012).  $D_R$  heterogeneity can result from variations in grain size or mineralogy, beta radiation microdosimetry on the millimeter scale (Mayya et al., 2006), and gamma radiation on the decimeter scale (Aitken, 1989).  $D_R$  modeling can account for non-ideal scenarios to some extent, but this requires a good understanding of the distribution of radioelements in the surrounding sediments and rocks (Martin et al., 2018). Temporal variations in the  $D_R$  (e.g., fluctuations in the water content or additions or losses of mineral phases due to weathering, pedogenic precipitation, or leaching) are challenging to quantify. Therefore, deposits that have undergone considerable soil development and weathering, or those from settings with highly variable water content, should be avoided. Uncertainty in the  $D_R$  will be greater in these cases and will influence the precision and accuracy of ages.

## Collecting Samples for $D_E$ Determination

Reviews and sample collection guides for luminescence dating are available elsewhere (Duller, 2004, 2008a; Gray et al., 2015; Nelson et al., 2015; Wintle and Adamiec, 2017; Bateman, 2019), so we only present a brief review of the essential sample collection steps here.

After careful assessment of the most suitable materials for dating (as described above), the main considerations are the most appropriate methods for collecting a light-safe sample for  $D_E$  analysis and representative samples or field measurements for  $D_R$  assessment. It is worth stressing that all sample processing is done in a dark-room setting with low-level red or amber light, like that used for processing photographic film (e.g., Sohbaty et al., 2017). Under red light lamps, anything written in red ink will not be visible in a luminescence laboratory. Additionally, laboratories usually do not have the mechanical equipment required to cut metal pipes. If metal end caps become stuck during sample collection, they will be difficult to remove for sample extraction in the labora-

tory; tape or flexible rubber or plastic endcaps are recommended.

Sediment samples for  $D_E$  analysis can be taken from exposed stratigraphic sequences by gently hammering an opaque tube horizontally into the target sediments (Fig. 3). The tube dimensions are generally ~20 cm long and between 4–6 cm in diameter but can be varied to conform to the thickness of the sedimentary unit, though sufficient material must be collected to isolate the target mineral and grain size needed for analysis (Bateman, 2015). It is also possible to collect samples from cored sediments and rocks (Nelson et al., 2019), although it is recommended to collect two cores, one to review the core stratigraphy and the other kept light-safe for sample collection. When the sample tubes are removed from the profile or core, the ends need to be covered by tape or aluminum foil and a secure cap to prevent light exposure and the mixing of grains during transport. At the laboratory, the outer 2 cm of sediment from the ends of the tube will be extracted for  $D_R$  analysis, and the innermost sediment will be processed for luminescence measurements. On-site measurements and representative samples for  $D_R$  determination should be collected from all sediments within 30 cm of the sampled intervals (see next section for details).

If the sediments are too compact or cemented to drive a tube into, a consolidated block of material can be manually extracted from the profile and wrapped with black plastic or aluminum foil and secured with tape to protect from light and keep the block intact. In the darkroom of the luminescence laboratory, the outer part of the block will be removed (~3–5 cm on each side, depending on the degree of compaction and presence of cracks), and the inner part that has not been exposed to daylight will be used for the  $D_E$  measurements.

In cases where the stratigraphic sequence contains clast-supported pebbles or larger rocks and it is impossible to insert tubes to collect matrix sediment, samples can be collected using dim, filtered red lights (typically around 590 nm) at night or under an opaque tarp. In this case, the outer 5 cm of the sediment profile that was previously exposed to light should be removed once under dark conditions, and the sample should then be collected in an opaque container and securely wrapped. Note that it is important to describe, photograph, and assess sample sites in the light prior to sampling under dark conditions. Sites should be reassessed for the quality and character of the materials sampled in the daylight following tarp removal or the next day to ensure that the most suitable sample was collected.

The last exposure of a rock surface to light can be dated using the novel rock surface dating

technique described by Sohbat et al. (2011). The advantage of this technique compared to conventional sediment dating is that information on the prior bleaching history of the rock is preserved in its luminescence depth profile. Applications include dating rock fall and cobble transport (Chapot et al., 2012; Liu et al., 2019), anthropogenically placed rocks and structures (Liritzis et al., 2013; Feathers et al., 2015; Mahan et al., 2015), or rock surface exposure to heating and fire (Rhodes et al., 2010). Rocks from these settings should be collected under dark conditions and wrapped in light-proof materials for transport. The side of the rock or block to be dated should be clearly labeled so it can be cored or sub-sampled in the laboratory.

Some sample types such as ceramics, burned flint, and fire-modified rocks may have received sufficient heat to reset the luminescence throughout the interior of the sample (Feathers, 2003). For these samples, the inside of the specimen will be used to determine  $D_E$ , and it is less important to prevent light exposure during sampling, but as with all samples, exposure to heat must be avoided. Many archaeological samples have been collected based on surface context or were previously collected and archived in museum collections, necessitating extra attention to the removal of light-exposed outer portions of the samples. Care should be taken, however, with siliceous materials such as flint or chert because they can be relatively transparent to light. Such samples should be placed in a light-free container upon excavation.

New advances in luminescence techniques have allowed for thermochronological applications related to characterizing rates of erosion and tectonic exhumation of rocks

(Guralnik et al., 2010, 2015; King et al., 2016). Sampling for these applications is similar to other rock collection methods, and light exposure should be avoided, or large enough samples should be collected to allow for the removal of the outer ~2–4 cm of the rock surface. Following collection, all samples for luminescence analysis should be stored safely to protect from additional exposure to light or heat.

### Required Samples and Measurements for Dose-Rate ( $D_R$ ) Determination

Considerations for measurement and calculation of the radiation dosimetry, water content, and cosmogenic dose rate are covered later in this paper. This section outlines field sampling approaches and requirements.

The  $D_R$  is the denominator of the age equation and is equally important as the numerator, the  $D_E$  (see Equation 1). To appreciate the components needed to determine the  $D_R$ , it is important to understand the travel range of different types of ionizing radiation (Fig. 6). Alpha radiation ( $\alpha$ ) is short ranged, traveling ~20  $\mu\text{m}$  in sediments, and is only significant if the internal radioactivity is from U and Th (Aitken, 1989). Its contribution to the  $D_R$  of sand-sized quartz is commonly disregarded because acid-etching steps during processing remove the outer rim of grains that would be affected by external alpha radiation. Grains with internal radioactivity, such as K-rich feldspars, and the associated increased U and Th contents will need to include alpha radiation contribution to the sample dose rate. Beta radiation ( $\beta$ ) affects sediment within a short distance of the radionuclide (~3 mm range in sediments). If the sample is in contact with material with dif-

ferent levels of radioactivity, such as a different sediment type beneath or near a rock, the beta dose from the other medium will also need to be known. Gamma radiation ( $\gamma$ ) has a range of ~30 cm in sediments and is largely derived from material outside the sample used for  $D_E$  estimation. In the field, photos, sketches, and notes should be made that describe the distance from the sample to different layers and clasts to accurately determine the gamma  $D_R$ . Because the relationship exponentially decreases with distance, materials closer to the sample will provide more gamma radiation than materials further away. In situ measurements may be important for accurate gamma  $D_R$  determination of heterogeneous environments.

A representative sample of the sediment within 30 cm of the  $D_E$  sample should be collected in a 1 L (quart sized) plastic bag and does not require light-proof handling. Once in the laboratory, the samples will be dried and gently disaggregated. It is important that samples are homogenized and scientific splits of the material are made using a sediment splitter to ensure that representative samples are analyzed. Note that a bulk sample will be accurate only if the environment around the sample is homogeneous. If it is not, a portion of each component within 30 cm of the sample will need to be collected and notes taken on the proportion and distance from the sample (see Fig. 6). Because of such complexity, it is common to measure the gamma  $D_R$  directly in the field using a portable gamma spectrometer or by leaving a luminescence-sensitive dosimeter in the sample location for up to a year. While preferable in some situations, such field measurements are not foolproof. It is difficult for the dosimeter and gamma spectrometers

Dose Rate component	[U]	[Th]	[K]	[Rb]	$\alpha$ -efficiency ( $k$ )	$\beta$ -attenuation ( $x$ )*	Pore-space $H_2O$	Burial depth	Geographic position (Elevation, Lat/Long)
alpha ( $\alpha$ )	✓ <sub>internal</sub> external	✓ <sub>internal</sub> external			✓	✓	✓		
beta ( $\beta$ )	✓ <sub>external</sub>	✓ <sub>external</sub>	✓ <sub>internal</sub> external	✓ <sub>internal</sub> external		✓	✓		
gamma ( $\gamma$ )	✓	✓	✓				✓	✓	
cosmic ( $c$ )							✓	✓	✓

\* $\beta$ -attenuation as function of grain-size

Coarse-grain quartz:

$$\text{Total } D_R = (x D_{R\beta} + D_{R\gamma} + D_{Rc})$$

Coarse-grain feldspar:

$$\text{Total } D_R = (k D_{R\alpha_{\text{int.}}} + k D_{R\alpha_{\text{ext.}}} + x D_{R\beta_{\text{int.}}} + x D_{R\beta_{\text{ext.}}} + D_{R\gamma} + D_{Rc})$$

Fine-grain silt:

$$\text{Total } D_R = (k D_{R\alpha_{\text{int.}}} + k D_{R\alpha_{\text{ext.}}} + D_{R\beta_{\text{int.}}} + D_{R\beta_{\text{ext.}}} + D_{R\gamma} + D_{Rc})$$

Scale of influence on  $D_R$ :

$\alpha$  = micron (internal and external  $D_\alpha$ )

$\beta$  = centimeter (internal and external  $D_\beta$ )

$\gamma$  = decimeter (external  $D_\gamma$ , 30 cm max)

Attenuation of radiation with distance from  $D_E$

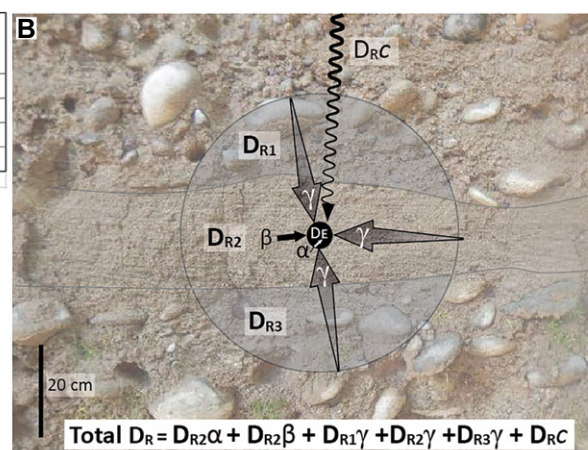


**Figure 6.** (A)  $D_R$  factors and calculation overview for coarse-grained quartz (63–250  $\mu\text{m}$ ), coarse-grained feldspar (63–250  $\mu\text{m}$ ), and fine-grained silt (4–11  $\mu\text{m}$ ) dating are shown. (B) Example of heterogeneous dose-rate environment within 30 cm radius of an optically stimulated luminescence/infrared stimulated luminescence (OSL/IRSL)  $D_E$  sample. Beta and gamma radiation attenuates with distance away from the sample location (see Aitken, 1998, for details).

to fit exactly into the same place as the extracted sample, which may be important for complex stratigraphy or a heterogeneous distribution of large rocks. Therefore, when possible, it is common to use both in situ and laboratory measurements to determine the  $D_R$ . High-precision laboratory measurements are preferred for beta  $D_R$ , while in situ measurements may better reflect the environmental gamma  $D_R$ .

Interstitial water radioactive element concentrations and water absorb radiation at a different rate than sediment. Higher water content in sediment and rocks translates into reduced radiation reaching the sample and a lower effective dose rate. Moisture content is determined using gravimetric methods and reported as weight percent of water in comparison to dry sediment. Water content can also be recorded as percent of saturation, and the saturation level of the sample can be determined experimentally in the laboratory or by using grain-size characteristics and expected porosity (Rosenzweig and Porat, 2015; Nelson and Rittenour, 2015).

Although water content can be measured directly from the sample to be dated, it is better to collect a separate sample in an airtight container to reduce moisture loss during transport to the laboratory. The water content sample should be collected from the back of the profile face to minimize the effects of desiccation. Information on seasonal changes in moisture as well as any long-term changes over thousands of years are important considerations when estimating time-averaged water content. However, it is most helpful to calculate saturation values and model changes over time in the laboratory (Rosenzweig and Porat, 2015) based on what is known about the long-term climate variability of the region. Usually large error terms, such as 20% of the measured value, are attached to the moisture values to account for such changes. The climate zone and sediment grain-size distribution can be used to estimate the typical field capacity of shallow sediments (Nelson and Rittenour, 2015).

The contribution from incident cosmic radiation also needs to be estimated to calculate the total  $D_R$  of a sample. This is calculated based on the depth of the sample below ground surface, along with the latitude, longitude, and altitude of the sample location (Prescott and Hutton, 1994). The time-averaged sample depth (converted to overlying sediment mass) is an important consideration and may not be the same as the sample depth at the time of collection if there has been erosion or deposition at the site (Munyikwa, 2000; López and Thompson, 2012). The density of the overlying sediment mass (overburden in  $\text{g/cm}^3$ ) should also be noted as sample depth is not the only variable constraining cosmic  $D_R$ . Sample depth also affects the gamma dose

contribution if the depth is less than 30 cm. In most situations, the cosmic  $D_R$  is minor in proportion to the radioactivity of the surrounding materials (5%–10% of the total  $D_R$ ). However, the cosmic dose and changes in burial depth can be significant in low  $D_R$  settings ( $<1$  Gy/kyr). Notes on changes in sample depth in sedimentary environments and cosmic shielding in cave and rock shelter settings are needed to accurately calculate  $D_R$ .

## LABORATORY SUBMITTAL AND PROCESSING

### Sample Shipment

Measures to securely package samples for air or ground travel should be taken to ensure safe handling during transport. First, sediment within sample tubes must be packed full so that sediment does not shift within the tube. Movement of grains may mix light-exposed sediment at the ends of the tube with the target material used for dating and could render the sample undatable unless care is taken to shield the entire process from sunlight. Clear notes should be included if the sample tube is stuffed with extra packing material on the ends (this can save time and effort in the laboratory). Second, sediment collected for  $D_R$  analysis should be double or triple bagged to prevent ripping and the loss of material. All sample components must be well-marked, clearly labeled with a permanent black or blue marker, and preferably not labeled only as OSL-1, -2, etc., as this can lead to confusion and duplication at the laboratory. We recommend covering labels with clear packing tape to prevent them from wearing off. Double check all labels, sample information sheets, and contents for consistency prior to submittal to the laboratory.

For packaging durability, do not ship in non-reinforced cardboard. Luminescence sample tubes and  $D_R$  samples are heavy and cause thin cardboard boxes to rip open. If shipping in cardboard boxes, use smaller boxes and fewer samples per box to keep the weight down. Hard-sided containers, such as small coolers, buckets, and toolboxes with lids taped shut, better protect samples during transport.

In addition to protecting  $D_E$  samples from light and heat exposure following collection, it is also important to ensure that samples are not subjected to prolonged contact with radiation sources (from scanning devices or strong X-rays) during transport and shipment to the laboratory. However, the dose given from these sources is usually small enough that it is only of concern for very young samples (i.e.,  $<0.1$  ka). Note that permits are often required for import

from foreign countries to avoid the destruction of samples and confiscation. Always contact the laboratory prior to sample submittal and forward all courier and tracking information so that laboratory personnel can help track your package and ensure its arrival at the intended destination.

### Sediment Processing

Once the samples reach the luminescence laboratory, they will be inventoried and given a unique laboratory identifier, opened, and processed under dim amber or red light ( $\sim 590$  nm) conditions, and mineral grains will be purified using physical and chemical treatments (e.g., Wintle, 1997). Depending on the target mineral, quartz and/or K-rich feldspar (orthoclase, microcline, and sanidine) grains will be isolated by either wet or dry sieving to a narrow grain size fraction between  $63\ \mu\text{m}$  and  $250\ \mu\text{m}$  for sand dating and  $30\text{--}63\ \mu\text{m}$  or  $4\text{--}11\ \mu\text{m}$  for silt dating. Target grain sizes are then treated with 10%–30% hydrochloric acid (HCl) to remove detrital carbonate, post-depositional carbonate coatings, and/or other acid-soluble salts. Organic materials are removed using hydrogen peroxide ( $\text{H}_2\text{O}_2$ ). A Frantz magnet separator is often employed to remove high iron content minerals in several passes at progressively higher amperage, which can also help to remove some of the calcium-rich feldspars. Higher density minerals are separated using water-soluble sodium polytungstate or lithium metatungstate for quartz ( $\rho = 2.7\ \text{g/cm}^3$ ) or K-rich feldspar ( $\rho = 2.58\ \text{g/cm}^3$ ). To clean quartz and remove the feldspar (or any lingering surface contamination), the  $<2.7\ \text{g/cm}^3$  subsample is treated with either 30% fluorosilicic acid ( $\text{H}_2\text{SiF}_6$ ) or 40%–50% hydrofluoric acid (HF) to remove feldspar minerals, followed by  $\sim 30\%$  HCl to remove fluoride precipitates that can form during HF acid digestion. The HF step also etches the outer few micrometers of the quartz grains to remove dose from alpha radiation and surface impurities such as iron oxides. Finally, samples may be re-sieved to remove finer sized fractions of etched quartz and any partially dissolved feldspars.

### Pottery Processing

For luminescence dating of pottery, the minimum recommended size of a sherd is  $15 \times 15\ \text{mm}$  and 5 mm thick (Ideker et al., 2017). Nearly all of the material of this size submitted to the laboratory will be expended during processing and analysis. Thicker and larger sherds are preferable as they may be subsampled with some material returned to the archive. In the laboratory, a low-speed drill is used to remove the outer 2–3 mm of material exposed to light



during collection (e.g., Spencer and Sanderson, 2012). Note that decorated pottery with textures and imprints may need to have more material removed to extract all light-exposed material. The material removed from the outer part of the sherd can be analyzed as part of the  $D_R$  sample, along with sediment or soil that the sherd was originally found within or near. Samples for  $D_E$  analysis will be derived from the inner portion of the sherd following gentle disaggregation and sieving. Quartz sand fractions extracted from the sherd will be purified using HCl and HF as described above for sediment processing. Silt from the pottery matrix (paste) is treated with dilute HCl and isolated using gravity separation (e.g., Feathers and Rhode, 1998; Feathers, 2009).

### Rock Processing

Rock surfaces can be analyzed to determine burial ages or exposure duration by developing a profile of luminescence versus depth back from the rock surface (Sohbati et al., 2011; Simms et al., 2011). This is mandatory for exposure dating because the shape of the profile relates to the age, but it is also useful for burial dating to gauge sufficient bleaching prior to burial. Sampling is usually done with diamond tipped core bits and a drill press in a light protected area. The cores are then cut into  $\sim 1$  mm slices with a precision diamond or water-cooled saw. The grains from the rock slices can be disaggregated and measured as single or multi-grain aliquots (Simms et al., 2011; Sohbati et al., 2011), or the rock slices can be directly measured on a conventional reader or imaged using a reader equipped with a digital camera mount if spatial information is required (e.g., Sohbati et al., 2011; King et al., 2019; Sellwood et al., 2019). The last exposure of a rock surface to heat can be assessed using a technique similar to that applied to ceramics, but because of steep thermal gradients, the center of the rock may not have been heated sufficiently. Single-grain dating may be necessary to separate heated from non-heated grains (Brown et al., 2018).

### LUMINESCENCE MEASUREMENTS AND ANALYSIS

Each luminescence laboratory has different instrumentation capabilities and specialties. What follows is an outline of the most common protocols and instrumentation for optical dating. More specialized equipment is used in emerging applications and to characterize luminescence physics and mineral properties (DeWitt et al., 2012). Examples of commercially available luminescence instruments originate from either DTU Physics in Denmark (Risø readers) or Freiberg Instruments in Germany (Lexsyg readers).

All luminescence instruments used for dating are equipped with light sources (light-emitting diode [LED] or laser), heating stages, photomultiplier tubes, filters for signal detection, and a radiation source (see Bøtter-Jensen et al., 2000; Richter et al., 2013).

Luminescence dating is an iterative technique that requires multiple measurements per sample over days to weeks to administer laboratory doses that are designed to replicate geologic doses. An aliquot is a sub-sample of one to thousands of quartz or K-feldspar grains mounted on  $\sim 1$  cm diameter discs or cups that are made of stainless steel, aluminum, or brass (generally for TL measurements). Grains can be mounted on discs with a silicon adhesive spray or placed in specially designed and precision-drilled, single-grain discs (Bøtter-Jensen et al., 2000). Tens to thousands of aliquots/grains are analyzed to calculate ages for each sample.

Purified quartz samples are typically stimulated with blue-green light ( $\sim 450$ – $525$  nm), and the resultant luminescence signal is detected through a UV wavelength filter while the sample is held at an elevated temperature of  $125^\circ\text{C}$  to isolate geologically stable luminescence signals. The resultant luminescence signal is calculated by subtracting the average of the background signal from the initial (fast) component of the signal decay curve (Murray and Wintle, 2003).

Feldspar samples are typically stimulated with infrared (IR,  $\sim 850$  nm) light, and the resultant luminescence signal is measured through blue wavelength filters. Infrared stimulated luminescence (IRSL) measurements are made at  $50^\circ\text{C}$  or using elevated-temperature, post-IRSL, or isothermal IRSL to circumvent or reduce the effects of anomalous fading or signal loss over time (Thomsen et al., 2008; Buylaert et al., 2009; Li and Li, 2011; Lamothe et al., 2020; Zhang and Li, 2020).

Single-grain dating is usually performed on quartz sand with a green laser (maximum energy fluence rate of  $\sim 50$  W/cm<sup>2</sup> at  $\sim 530$  nm; Duller et al., 1999) or on feldspathic sand with an infrared laser (maximum energy fluence rate of  $500$  W/cm<sup>2</sup> at  $\sim 830$  nm) using specialized, precision-drilled discs or with an electron multiplying charge coupled device camera and LED stimulation. Lasers used for single-grain measurements have a higher stimulation power density than the LED arrays used in small aliquot analyses; therefore, the stimulation time for single-grain dating is reduced to  $\sim 1$  s per grain per OSL measurement (as opposed to  $\sim 20$ – $100$  s for conventional LED stimulation). Due to the often low luminescence sensitivity of quartz (e.g., in some samples only  $\sim 5\%$  of grains

give detectable luminescence signals), hundreds to thousands of grains must be analyzed to produce an age (Duller, 2008b).

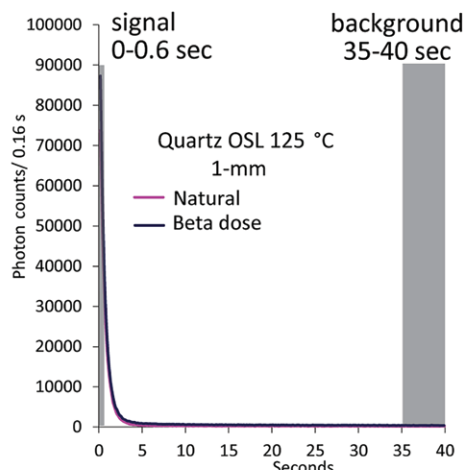
### Common Methods of $D_E$ Determination

Modern protocols for  $D_E$  determination have largely shifted away from the older thermoluminescence (TL) and multiple-aliquot techniques that were the mainstay of the technique in the 1970s to 1990s (Wintle, 2008). Today, common methods are focused on measurements using OSL and single-aliquot techniques on ever smaller aliquots. The field of luminescence dating has advanced considerably in the past 20 years following the formative development of the SAR methods for quartz (Murray and Wintle, 2000), feldspar (Wallinga et al., 2000), and single-grain dating (Duller et al., 2000). Newer developments in instrumentation (such as pulsed luminescence, e.g., Denby et al., 2006) and other innovative methods have led to expanded application of luminescence dating to older deposits (Jain, 2009; Porat et al., 2009; Lapp et al., 2009) and solutions for persistent problems with anomalous fading in feldspars (Buylaert et al., 2012; Kumar et al., 2021).

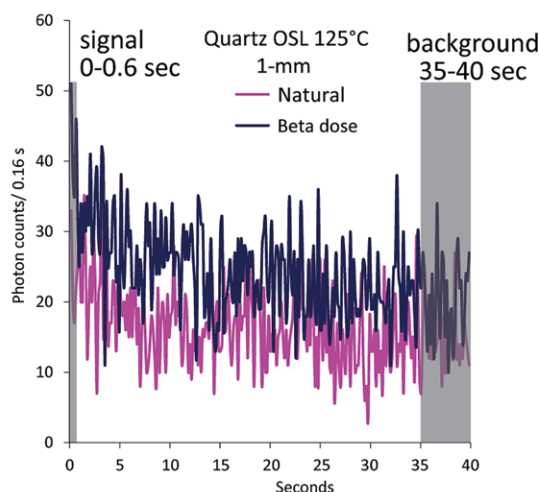
### SAR Methodology

Early efforts to produce single-aliquot methods for feldspar by Duller (1991) were refined for quartz by Galbraith et al. (1999) and Murray and Wintle (2000) to create the single-aliquot regenerative dose (SAR) method, which is now the most popular approach for quartz and feldspar dating. It involves the measurements of the natural signal ( $L_n$ ) and the luminescence from a series of (usually four or more) regenerative doses ( $L_x$ ) on an individual aliquot or grain. After each  $L_n$  and  $L_x$  measurement a fixed test dose is given and measured to account for sensitivity change between individual measurements. The sensitivity-corrected natural signal ( $L_n/T_n$ ) is interpolated onto the dose response curve (DRC) obtained by fitting the regenerative dose data ( $L_x/T_x$ ) with a given function (e.g., a saturating exponential function; Figs. 7–8). Generating the DRC is the time-consuming step, given that many aliquots or grains need to be measured, especially for old samples for which long laboratory irradiation times are needed to capture higher natural doses. In general, for multi-grain analyses of quartz,  $\sim 24$  aliquots are measured, while fewer aliquots can be measured for K-feldspar because they are brighter and generally produce lower  $D_E$  scatter. Single-grain analyses require a greater number of analyses ( $>100$  and up to several

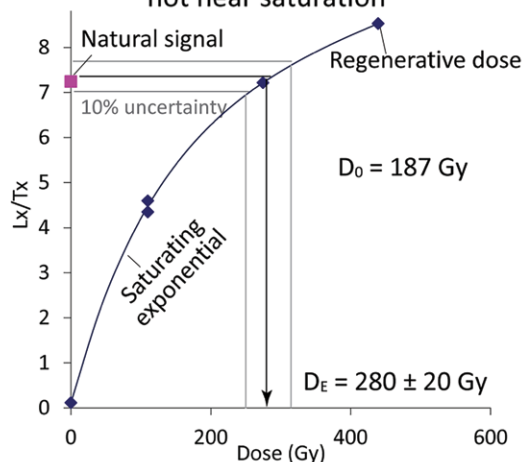
## A Luminescence Signal Decay high-sensitivity quartz:



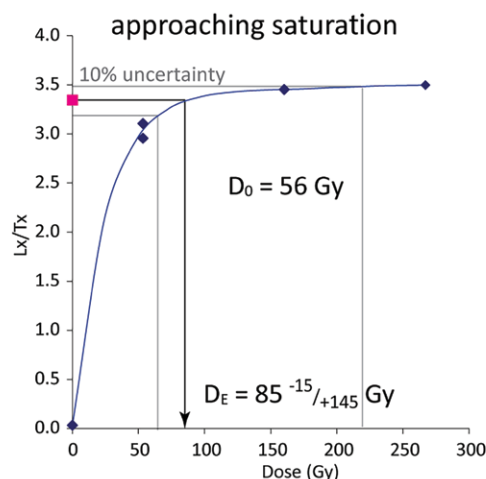
## B Luminescence Signal Decay low-sensitivity quartz:



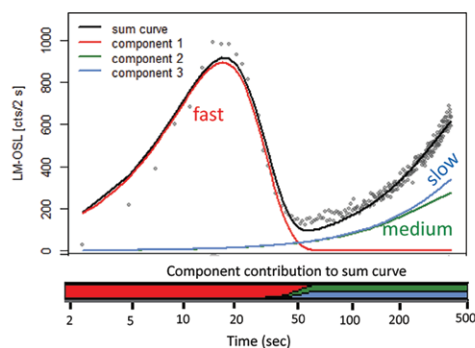
## C Dose Response Curve: not near saturation



## D Dose Response Curve:



## E Linear-modulated OSL



## F Thermoluminescence

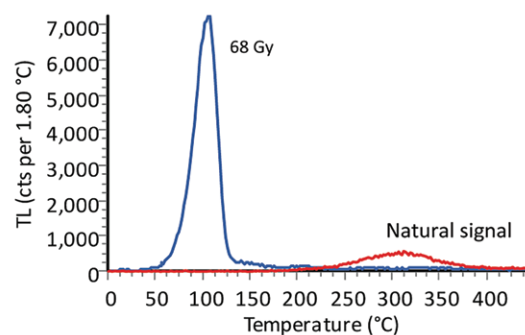


Figure 7. Characteristic quartz luminescence properties that are commonly supplied as supplemental data are shown. (A) Small aliquot (~10 grains) signal decay curve in response to blue light-emitting diode stimulation for a sample of relatively high-sensitivity quartz. This sample would appear as a green dot ( $>1000$  counts/Gy/mm<sup>3</sup>) on the quartz luminescence sensitivity map (Fig. 5). (B) Small aliquot (~10 grains) signal decay curve for a sample with low-sensitivity quartz. This sample would appear as a red dot ( $<250$  counts/Gy/mm<sup>3</sup>) in Figure 5. (C) Dose response curve (DRC) for a sample with a natural dose that is lower than the suggested  $2 \cdot D_0$  limit for maximum  $D_E$  calculation.  $D_0$  is the characteristic dose of saturation on a DRC, where exposure to higher radiation does not produce a linear increase in luminescence signal. (D) DRC where additional laboratory irradiation above 56 Gy does not produce a linear luminescence response. Uncertainty on the  $D_E$  is high and asymmetric due to the interpolation of the natural sensitivity-corrected signal ( $L_n/T_n$ ) onto a saturating DRC in the high dose region. (E) Linear modulated–optically stimulated luminescence (LM-OSL) signal displays multiple luminescence components of a quartz multi-grain aliquot. LM-OSL measurements are conducted using linearly ramped light intensity and the luminescence code package in R to model fast, medium, and slowly decaying luminescence components. The fast-decay component is best suited for OSL dating. (F) Quartz thermoluminescence (TL) glow curves. The 110 °C TL peak

shown for laboratory doses is unstable in nature, and this signal is cleared with a preheat prior to OSL measurement and kept empty by holding at 125 °C during measurement (Murray and Wintle, 2000).

thousand) due to greater grain-to-grain scatter and weak luminescence signals. Common data quality and reproducibility checks for SAR results include recovery of an applied dose

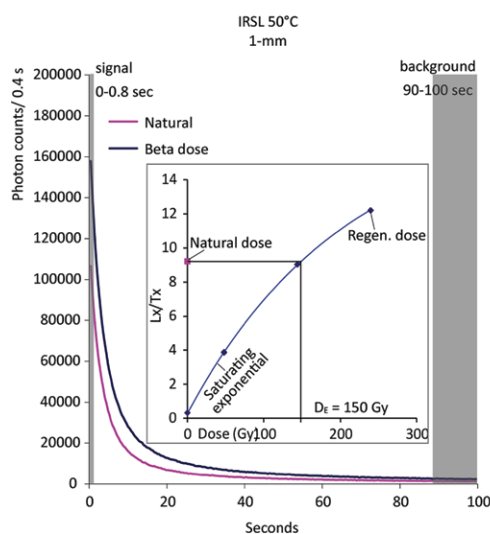
and a check on the influence of the pre-heat temperature of resultant  $D_E$  values (so-called dose-recovery and pre-heat plateau tests, e.g., Wintle and Murray, 2006).

## Feldspar IRSL and post IR-IRSL

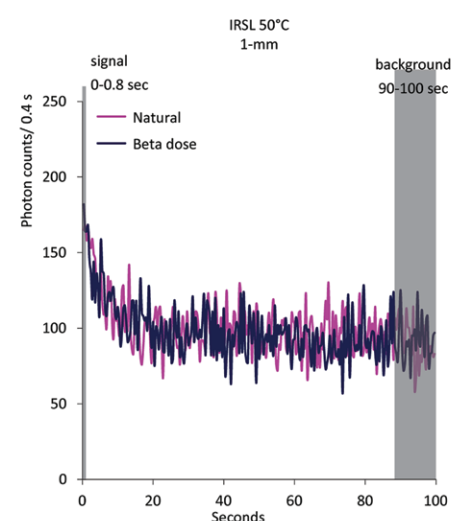
Dating with quartz dominates the published literature, but advances in IRSL methods in



### A Luminescence Signal Decay high-sensitivity feldspar:



### B Luminescence Signal Decay low-sensitivity feldspar:



### C Fading Test

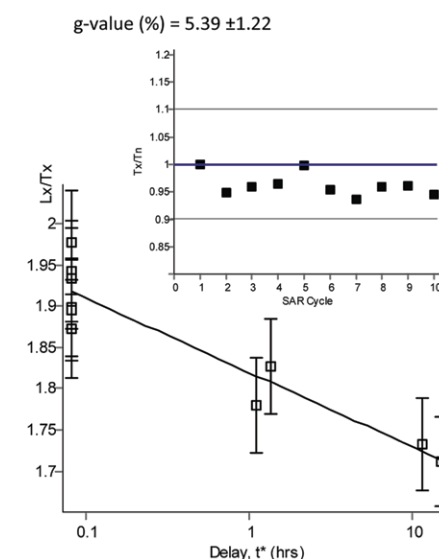


**Figure 8.** Characteristic feldspar luminescence properties are shown. (A) Luminescence Signal Decay: high-sensitivity feldspar IRSL 50 °C on 1-mm small aliquot (~10 grains). The inset dose response curve is well below saturation. (B) Luminescence Signal Decay: low-sensitivity feldspar IRSL 50 °C on 1-mm small aliquot (~10 grains). (C) Fading Test results of nine sensitivity-corrected dose cycles with varying measurement delays following Auclair et al. (2003).

recent years have renewed interest in feldspar dating. Feldspars are an important mineral for luminescence dating because they often produce brighter signals than quartz (which can suffer from low sensitivity), and feldspar saturates at a higher  $D_E$  level, which allows older deposits to be dated (Fig. 8). Luminescence dating of feldspars has had a rocky past, but improvements have been made in recent decades. TL dating of K-feldspars was common in the early 1970s (Mejdahl, 1972, 1985); however, progress slowed when it was discovered that ages of volcanic and other deposits were underestimated due to anomalous fading (Wintle et al., 1971; Wintle, 1973; Huntley and Lamothe, 2001). Modern analyses use IRSL, and methods have been developed to correct feldspar ages for anomalous fading (Huntley and Lamothe, 2001; Lamothe et al., 2003; Kars and Wallinga, 2009). Approaches using elevated-temperature stimulation following low temperature IRSL (post-IR IRSL) and multiple elevated temperature post-IR stimulation (MET post-IR IRSL) have also been developed to exploit more stable luminescence signals (Thomsen et al., 2008; Li and Li, 2011). More recent methods in development seek to overcome the fading problem by looking at different luminescence production processes (Frouin et al., 2017b; Kumar et al., 2021) or by using a post-isothermal signal (Lamothe et al., 2020).

### Portable Luminescence Readers

Exciting new prospecting tools such as portable luminescence readers offer relatively quick and easy measurements and adapt well to in situ field measurements (Bøtter-Jensen et al., 2010).  $D_E$ ,  $D_R$ , and age estimates in the field are not currently possible due to the need for an ionizing radiation source that does not induce health hazards. Nonetheless, in areas with homogeneous  $D_R$  conditions and minimal variation in the sediment provenance (i.e., no large changes in quartz or feldspar sensitivities), a portable luminescence reader can provide relative differences in natural luminescence signals between samples and help identify stratigraphic breaks or unconformities within a deposit. When coupled with full laboratory-generated luminescence age results, the signals from portable readers can be converted to modeled ages and provide information on deposition rates, approximate age and duration of deposition, and whether the deposits fall within the applicable range of luminescence dating (Sanderson and Murphy, 2010; Gray et al., 2018; Munyikwa et al., 2021; DuRoss et al., 2022). Results can also provide information on bleaching processes and sediment transport. Sampling guided by the portable reader makes it possible to translate the lateral distribution of luminescence signal intensities

into sediment migration/transport rates (Gray et al., 2017, 2019; Liu et al., 2019).

Portable reader measurements of luminescence characteristics both laterally as well as in a stratigraphic section can also provide information on past changes; this is not possible with traditional proxy environmental indicators (Mendes et al., 2019). It is possible to use measured luminescence characteristics from a portable reader by obtaining the shape of the OSL or TL signals or sensitivity as a tracer for sediment provenance on a basin scale over any geological time scale. These characteristics are most likely linked to the origin of the source rocks from which quartz or feldspar were derived, degree of weathering, erosion, and transport history of each grain (Sawakuchi et al., 2018).

### DOSE-RATE MEASUREMENTS AND CALCULATION

Ionizing radiation comprising the environmental  $D_R$  originates from the radioactive decay of  $^{40}\text{K}$  (beta and gamma) and the decay series chains of  $^{238}\text{U}$ ,  $^{235}\text{U}$ , and  $^{232}\text{Th}$  (alpha, beta, and gamma) and, to a lesser extent,  $^{87}\text{Rb}$  (beta only) (Fig. 6). It is assumed that the distribution of radioelements surrounding a sample is homogeneous, and the spatial dimensions of the surrounding medium are greater than the range of radiation, which is also known as infinite matrix

assumption (in sediments, this is typically ~30–50 cm for gamma rays; Guérin et al., 2012).

Methods for  $D_R$  analysis vary between laboratories but are largely grouped into spectrometry and geochemistry methods. Laboratory-based analysis of radio-elemental activity or concentration can be assessed using gamma spectrometry, neutron activation analyses, alpha and beta counting, atomic emission, X-ray fluorescence, inductively coupled plasma–mass spectrometry (ICP-MS), and ICP–optical emission spectrometry (ICP-OES) analyses. In situ gamma spectrometers or buried  $Al_2O_3:C$  dosimeters can be used for field-based environmental dose rate, laboratory-based high-resolution gamma spectrometry. This is an important method for  $D_R$  determination because it allows the quantification of radioelements and daughter products critical for  $D_R$  calculation, which can be used to detect possible radioactive disequilibria. Variations in radioactivity over time may occur when soluble minerals or elements such as  $^{238}U$  or  $^{226}Ra$  are transported by water or gas diffusion of  $^{219}Rn$ , leading to the addition or loss of radioisotopes (Olley et al., 1996). In contrast, ICP-MS is cheaper and quicker, but it only allows the determination of parent radioelements of  $^{238}U$  and  $^{232}Th$  and thus assumes secular equilibrium in the decay chains (ICP-OES is used for  $^{40}K$ ). The small amount of material analyzed may cause non-representative results if samples are not homogenized or collected in a representative fashion in the field, necessitating repeat analyses of subsamples to confirm the results.

Environmental dose-rate conditions vary considerably between samples, but in most cases they are in the range of 1–4 Gy/kyr for quartz and ~30–50% higher for K-feldspars due to the additional contribution from the internal dose rate. Beta decay from  $^{40}K$  is generally the greatest contributor of beta radiation to the  $D_R$ , and beta radiation contributes more than gamma radiation to the total  $D_R$  (the typical contribution for coarse-grained quartz samples is 65% from beta and 30% from gamma, with the rest coming from cosmic radiation and internal  $D_R$  (Ankjaergaard and Murray, 2007)).

### Cosmogenic Dose and Interstitial Water Content

For most samples, a small portion of the total accumulated dose is delivered by cosmic particles (often <10%; Preusser et al., 2008). The cosmogenic  $D_R$  is calculated based on sample geolocation data and the mass of overlying material, which is typically converted to burial depth based on the density of the overlying materials. If samples are collected from depths exceeding ~50 cm, an estimate of the hard component of

the cosmogenic  $D_R$  is calculated based on the sample geolocation (longitude, latitude, and altitude) and overburden depth (Prescott and Hutcheon, 1994). For shallow (<~50 cm) or surface samples, the interplay of the soft component (Prescott and Stephan, 1982) should be considered (Rhodes et al., 2010).

In settings with very low environmental radioactivity, for example, where fluvial systems drain highly weathered ancient cratons and have deposited quartz-rich sediments (Guedes et al., 2017; Spencer et al., 2019), or in carbonate tufas (Ribeiro et al., 2015), the cosmogenic  $D_R$  becomes significant, and it must be estimated accurately. In situ measurements can be achieved by recording events above 3 MeV using a portable spectrometer (Aitken, 1985) of the type normally used to record field gamma activity, or with the use of on-site dosimeters. Variation between full  $4\pi$  to surface  $2\pi$  gamma geometry effects (Aitken, 1985) must also be assessed concurrently.

It is necessary to correct external  $D_R$  for estimated water content between sediment grains to calculate the effective  $D_R$  for a sample. Field gravimetric moisture content (mass of moisture/mass of dry sample) is simple to measure by recording representative sample mass before and after drying a sample in an oven. A common procedure is to assume the field moisture measurement represents the stable interstitial water content of the sampled medium over the burial period and compare this value to estimates of saturated water content. The climate regime and grain size of a sample can be used to inform the field capacity of the sediment to hold water and derive a suitable uncertainty estimate (Nelson and Rittenour, 2015). Caution should be taken when interpreting in situ water content due to effects from the drying of outcrops, changes in climate and water table, and sediment compaction over time (Mahan and DeWitt, 2019; Ashley et al., 2017). A possible range of water contents should be used based on available environmental and paleoclimate data to estimate the average water content over the lifetime of the sample.

### Online $D_R$ Calculators

$D_R$  calculation is not mathematically complex, but many values and associated uncertainties need to be assessed to calculate the total internal and external environmental  $D_R$  of a sample (Durcan et al., 2015). The use of published calculators and calculation tools offers a straightforward method of  $D_R$  calculation and reduces the potential for errors. They also provide a way to compare different studies and inter-laboratory comparisons.

Non-commercial, peer-reviewed calculators are published that are aimed at straightforward  $D_R$  contexts where infinite matrix and radionuclide equilibrium assumptions can be made (Guérin et al., 2012). These include the Dose Rate and Age (DRAC) online calculator (Durcan et al., 2015), Java-based applications such as DRc (Tsakalos et al., 2016), DOS-based AGE (Grun, 2009), as well as self-written Anatol software (Gaugez and Mercier, 2012), Excel-based calculators including the Luminescence Dose and Age Calculator (LDAC; Liang and Forman, 2019), and the DRAC-based eM-AGE (Pérez-Garrido, 2020). In addition, DRAC can be used within the R Luminescence package (Kreutzer et al., 2020) and in the R TL dating package (for complex geometries and TL dating; Strebl et al., 2019). Within the R Luminescence package, there are other  $D_R$ -relevant functions, including the calculation of the cosmic  $D_R$  (Burow, 2020), the scaling of the gamma  $D_R$  (Riedesel et al., 2020), and a  $D_R$  calculation for cobble samples (Riedesel and Autzen, 2020). For  $D_R$  calculation in more complex environments, specialized software and modeling options are available. For example, DosiVox (Martin et al., 2018) is a Geant4-based software for dosimetric simulations of complex geometries, and the function “RCarb” (Kreutzer et al., 2019) offers the option for estimating dose rates in carbonate-rich environments (Nathan and Mauz, 2008). A more complete list of luminescence data analysis software is maintained on the Ancient TL website (<http://ancienttl.org/software.htm>).

## EXAMPLES OF DATA ANALYSIS AND DISPLAY

### Dose Distribution and Age Models

$D_E$  values are measured on multiple subsamples ranging in volume from single-grain to multi-grain aliquots. The adequate number of grains or aliquots used to evaluate the cumulative  $D_E$  varies in each study and depends on the geologic or archaeologic context. For example, if well-bleached samples with low overdispersion are analyzed, then ≤20 multi-grain aliquots may suffice. However, when dealing with partially bleached samples, the number and size of aliquots should be increased significantly (50 or more as proposed by Rodnight, 2008), or single grain measurements should be performed (typically hundreds to thousands of single grains are analyzed) (Feathers and Tunnicliffe, 2011).

These individual  $D_E$  results need to be combined statistically to obtain a representative  $D_E$  value for age calculation. Several statistical models can be used for this purpose. These are commonly referred to as “age models,” although they are, in fact, models for  $D_E$  calculation. An

exception to this is the correction for fading on feldspar; that correction is done on the age and not on  $D_E$ . Frequently used models are described below. The depositional and stratigraphic setting in which the sample has been collected as well as the number of measured  $D_E$  values need to be considered when selecting the most appropriate model for a setting. However, while attempts have been made to create formal age-model decision trees (Bailey and Arnold, 2006), there is no universal protocol for appropriate age-model choice. Therefore, it is important to present the criteria used for age-model choice and the  $D_E$  distributions to provide transparency in the choice of calculation.

Commonly used statistical methods for calculating  $D_E$  values range from the simple use of the mean or weighted mean to models with internal assumptions of  $D_E$  distributions, sediment bleaching, and scatter. The central age model (CAM, Galbraith et al., 1999) is best applied in settings where all grains were fully zeroed (bleached) at the time of the event to be dated (transport, fire exposure, fault rupture, etc.). The CAM treats the logged  $D_E$  distribution as normally distributed, and it produces an error-weighted average  $D_E$  value. This model allows the scatter beyond instrumental error in the data, which is known as overdispersion (i.e.,  $\sigma$  or OD), to be quantified. The Average Dose Model (ADM, Guérin et al., 2017) is, in some ways, similar to the CAM but assumes added  $D_E$  scatter due to beta  $D_R$  heterogeneity (microdosimetry) from the proximity of sensitive grains to hot spots. These localized (millimeter-scale) zones of higher-than-average  $D_R$  are due to the presence of K-rich feldspar or zircon and other U-rich mineral grains in the sediments. The choice of the CAM or ADM is based on information related to the cause of  $D_E$  scatter in a particular setting (e.g., Heydari and Guérin, 2018).

In samples that display non-normally distributed  $D_E$  values, a minimum age model (MAM, Galbraith et al., 1999) or finite mixture model (FMM, Roberts et al., 2000; Galbraith, 2005; Arnold and Roberts, 2009) may be used to discriminate between different  $D_E$  populations. The MAM uses initial parameters to fit a truncated normal distribution to the logged  $D_E$  data to calculate a statistical estimate of the minimum range of  $D_E$  values and is best suited to settings where not all grains were adequately bleached (reset) before burial (e.g., high-energy environments like fluvial and glacial deposits).

The FMM is best applied to settings with multiple  $D_E$  population modes due to post-depositional mixing and other processes leading to differential dose rate and burial history of grains. The FMM splits the  $D_E$  distribution into statistically different components and reports the

proportion of  $D_E$  values in each modeled population. The FMM should only be applied to single-grain distributions due to averaging effects from multi-grain aliquots (e.g., Arnold et al., 2012), but results can be used to understand grain-scale processes of sediment mixing, microdosimetry, and partial bleaching in a deposit (e.g., Duller, 2008b; Gliganic et al., 2016). While there is still debate over whether the  $D_E$  components identified by the FMM can reliably be used for age calculation, it can quantify grain dose distributions that are not necessarily linked to ages (Guérin et al., 2015, 2017). The FMM is useful for understanding the structure of  $D_E$  distribution data and for distinguishing grains with differing luminescence properties (e.g., Roberts et al., 2000; Gliganic et al., 2015; Smedley et al., 2019; Hu et al., 2020).

Figure 9 presents commonly used methods of plotting  $D_E$  data and highlights the estimated  $D_E$  values for CAM, MAM, and FMM for samples from different settings. The final choice of an age model for  $D_E$  calculation should be steered by the expected bleaching characteristics of the depositional setting, field evidence for post-depositional mixing, resulting  $D_E$  distribution, and  $D_R$  conditions. The number and type of analyses is also an important consideration because adequate data are needed for input to the chosen model. For example, the MAM and FMM are not suitable for a limited number of  $D_E$  estimates (Galbraith and Roberts, 2012) or for effective multi-grain measurements.

Keeping in mind the axiom, “all models are wrong, but some are useful,” (Box, 1976) it is recommended that radial plots (Galbraith, 1990), abanico plots (Dietze et al., 2016), or other data plots that include information on  $D_E$  distributions are included in publications to fortify the justification of the chosen age ( $D_E$ ) model (Fig. 9). Other methods for displaying individual dose distributions are probability density functions, kernel density functions, and histograms, though each come with their own set of visual biases due to malleable display parameters or peakedness based on  $D_E$  uncertainties.

### Sedimentation Rate and Mass Accumulation Rates

Luminescence dating has other perks aside from discrete age determination. It can be used to estimate sedimentation or mass accumulation rates in continuous lacustrine or loess deposits (Roberts, 2008; Stevens et al., 2016) and the evolution of laterally accreting systems (Tamura et al., 2019). A combination of high-density sampling and Bayesian analysis has been demonstrated to provide robust age-depth models (Combès and Philippe, 2017; Zeeden

et al., 2018; Perić et al., 2019; Fenn et al., 2020). Bayesian modeling can reduce overall uncertainty by simultaneously modeling the  $D_E$  distributions and the individual components of the  $D_R$  (Guérin et al., 2021) and can help clarify occasional age inversions in the chronostratigraphic data. The main advantage of luminescence age-depth models, compared to radiocarbon dating, is the larger time range accessible by the luminescence technique and the ability to date sediments void of organic material.

### DATABASES AND METADATA

Open access to scientific data is important for the exchange of information and for promoting scientific advancement across geochronologic fields and the greater Earth science community. Luminescence dating is data-rich and can provide useful information such as burial ages, transport history, dosimetry, and geochemistry. Researchers in search of easy-to-acquire bulk signals from Earth materials may use this type of data to model landscape evolution, human occupation, or to serve as a baseline for paleoclimate correlations (e.g., Singhvi and Porat, 2008; Wintle, 2008; Lai, 2010; Thomas and Burrough, 2016; Brown, 2020; Gray et al., 2020). Recent forums and vision statements sponsored by the U.S. National Science Foundation and the U.S. National Academy of Sciences have highlighted the importance of supporting access to geochronology resources and data, improving cyber-infrastructure for data storage, and sharing and diversifying human resources and training within geochronology fields (Harrison et al., 2015; NASEM, 2020).

Important to advancing science and achieving these goals is the development of open-access online databases. There is a growing need for such data repositories as funding agencies and government-supported research mandate data archiving. Moreover, while journals require documentation of supporting data, the maintenance of those data repositories is shifting away from the journals and to the researchers and their supporting organizations. Here we provide an outline of current resources available for archiving metadata and accessing previously collected results, though a centralized geodatabase for geochronologic data resources should be the ultimate goal. One example is the U.S. Geological Survey's ScienceBase site (Table 4; Gray et al., 2021).

There are many benefits to a centralized and open-access database for luminescence results and characteristics. For one, a centralized repository would archive information for researchers who want to quickly determine if past luminescence dating studies have been conducted in a geographic region, and if so, what dating

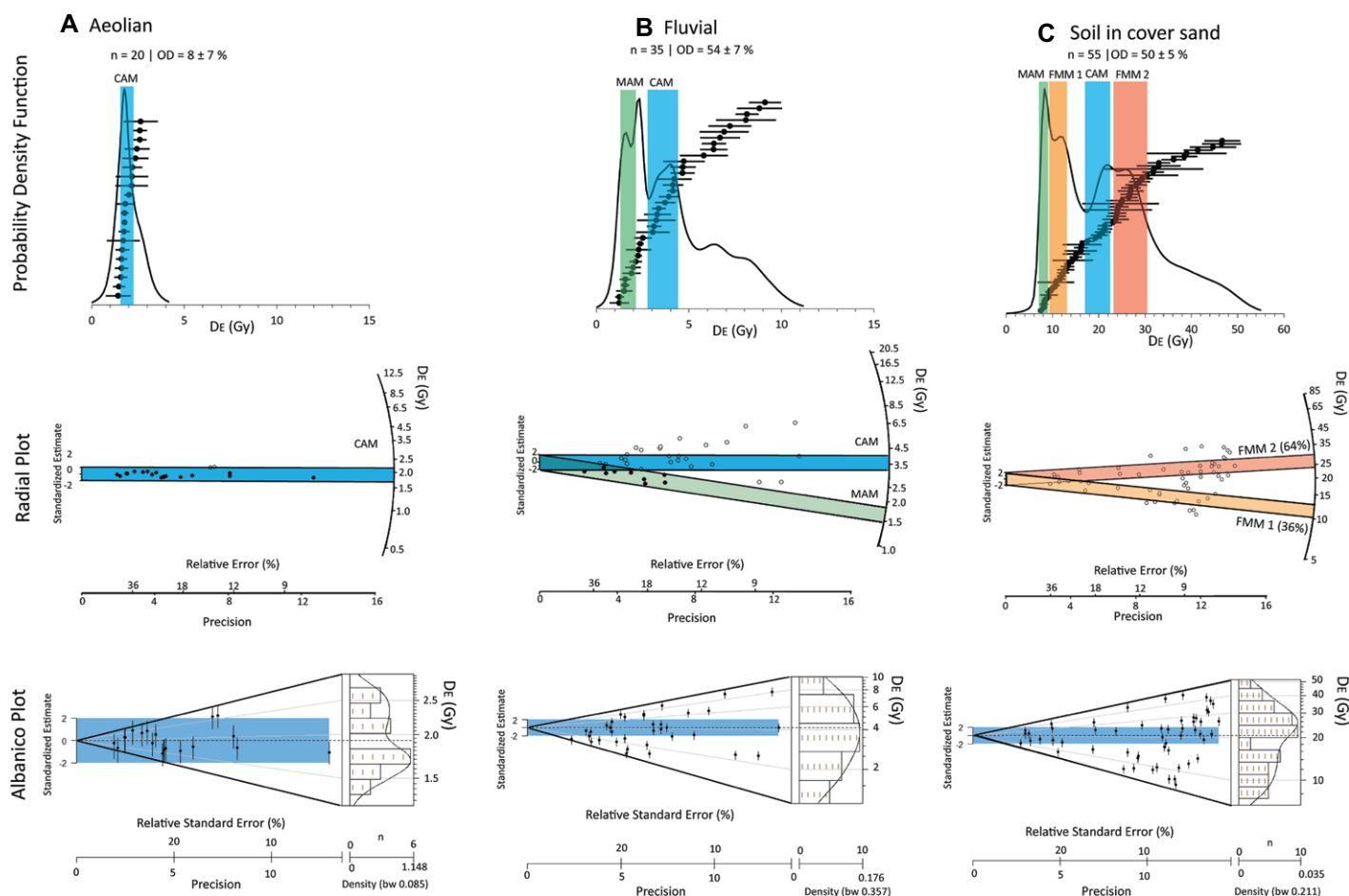


**Figure 9.**  $D_E$  data distribution plots include (top) probability density function, (middle) radial plot (Radial Plot v1.3 software), and (bottom) abanico plot (RStudio with the Luminescence package). (A) Small aliquot (~10 grains) data for an aeolian sand sample.  $D_E$  results cluster on their central value and are considered “well-bleached.” (B) Single-grain fluvial sand sample exhibits significant scatter in  $D_E$  values likely due to partial resetting of previous luminescence signals, and thus some grains contain a residual burial dose signal.  $D_E$  values most likely to have been reset during the last exposure event are selected using the minimum age model (MAM). (C) Single-grain  $D_E$  data of sample collected from cover sands impacted by soil development and bioturbation. The high likelihood of post-depositional mixing requires single-grain dating and finite mixture modeling. For this sample, a true burial dose is not likely to be estimated, so apparent ages and probability of  $D_E$  populations are selected. Blue shading represents the central age model (CAM), green shading represents the MAM, and orange/coral shading represents the finite mixture model (FMM) of Galbraith et al. (1999). Model input for overdispersion (OD) values was 0.3 in all MAM and FMM calculations.

approach has proven most reliable. While it is only a preliminary guide, Figure 5 is a useful example of the scale of variability in luminescence sensitivity and complexity. Data mining a centralized database would allow researchers to identify common problems with luminescence properties, focus laboratory experiments used to verify the suitability of a measurement protocol or mineral for dating (e.g., dose-recovery and preheat-plateau tests, etc.), and to identify landforms or stratigraphic units of old age (or high  $D_R$ ) in their study areas that might be beyond the range of luminescence techniques.

Several geochronological repositories focused on the Quaternary can be found online (Table 4), and each has its own focus. Nine of these include luminescence data, but only one database (the

Netherlands Centre for Luminescence Dating NCL Luminescence Data base or LumiD) is focused entirely on luminescence data. While most repositories link the sample data to its original scientific publication, luminescence data are reported in varying levels of detail. The NCL LumiD contains the most detailed template for luminescence data archiving, including final luminescence ages and errors,  $D_E$  and  $D_R$  values, sample grain size, sample preparation details, aliquot sizes, assigned age models, details regarding the sample site, and sampling processes.

Other databases, like Octopus, only include the mineral and measured signals in addition to basic luminescence data. Some archives allow online perusal using various search parameters or a clickable map (Neotoma and the U.S. Geological

Survey Science Base, see Table 4). AustArch and the INQUA Dunes Atlas consist of downloadable Excel sheets, the latter accompanied by a Google Earth kmz file. Sparrow (Neudorf et al., 2019b) provides a cyberinfrastructure for data storage and management at the laboratory level that facilitates the export of age data to larger, community-based repositories. CRC806 is perhaps the most complex repository as it houses a wide range of data types from archaeology, cultural sciences, and geosciences. However, luminescence data are displayed differently for each project and may include data tables or Excel sheets, written abstracts, reports, and publications.

Although current online repositories provide a means of accessing compilations of luminescence data, they vary widely with respect to

TABLE 4. EXAMPLE LIST OF EXISTING GEOCHRONOLOGICAL REPOSITORIES RELEVANT TO THE QUATERNARY

Repository (*includes luminescence data)	Geochronological Data	References
Netherlands Centre for Luminescence Dating LumiD* Database ( <a href="https://www.lumid.nl/LumiDB">https://www.lumid.nl/LumiDB</a> )	Luminescence ages	Davids et al. (2006)
Sparrow* ( <a href="https://sparrow-data.org/">https://sparrow-data.org/</a> )	Lab-specific, includes luminescence, cosmogenic, Ar-Ar, U-Th-Pb, Rb-Sr, and Sm-Nd geochronological data.	Neudorf et al. (2019b); Quinn et al. (2021)
OCTOPUS* ( <a href="https://earth.uow.edu.au/">https://earth.uow.edu.au/</a> )	Cosmogenic and luminescence ages in fluvial sediment.	Codilean et al. (2018)
Utah Geological Survey Geochronology Database* ( <a href="https://geology.utah.gov/apps/geochron/">https://geology.utah.gov/apps/geochron/</a> )	Ar ( $^{40}\text{Ar}/^{39}\text{Ar}$ ), thermoluminescence, infrared stimulated luminescence, and optically stimulated luminescence, tephro., fission track, terrestrial cosmogenic nuclides (TCN), tritium, $^{14}\text{C}$ , $^{87}\text{Rb}/^{87}\text{Sr}$ , or U-Th-Pb ( $^{238}\text{U}$ , $^{235}\text{U}$ , $^{206}\text{Pb}$ , $^{207}\text{Pb}$ ) ages.	
INQUA Dunes Atlas Chronologic Database* ( <a href="https://www.dri.edu/inquadunesatlas/">https://www.dri.edu/inquadunesatlas/</a> )	Luminescence ages.	Lancaster et al. (2016)
Strategic Environmental Archaeology Database (SEAD) ( <a href="https://www.sead.se/">https://www.sead.se/</a> )	Fossil insects, plant macrofossils, pollen, geochemistry and sediment physical properties, dendrochronology and wood anatomy, ceramic geochemistry and bones, dating methods.	Buckland (2014)
CRC806* ( <a href="https://crc806db.uni-koeln.de/start/">https://crc806db.uni-koeln.de/start/</a> )	Geoscientific samples of core/soil, archaeological site descriptions, dated artifacts, analyses of excavation profiles, published literature, public data of the spatiotemporal context of concern.	Willmes (2016); Willmes et al. (2018)
Neotoma Paleoecology Database* ( <a href="https://www.neotomadb.org/">https://www.neotomadb.org/</a> )	Fossil pollen, vertebrates, diatoms, ostracods, macroinvertebrates, plant macrofossils, insects, testate amoebae, geochronological data, organic biomarkers, stable isotopes, and specimen-level data.	Williams et al. (2018)
AustArch* ( <a href="https://archaeologydataservice.ac.uk/archives/view/austarch_na_2014/">https://archaeologydataservice.ac.uk/archives/view/austarch_na_2014/</a> )	$^{14}\text{C}$ , optically stimulated luminescence, thermoluminescence ages, oxidizable carbon ratio, uranium-series, electron spin resonance, cation ratio dating, and amino acid racemization ages.	Williams et al. (2014)
Wales and Borders Radiocarbon Database ( <a href="https://museum.wales/radiocarbon">https://museum.wales/radiocarbon</a> )	$^{14}\text{C}$ ages.	Burrow (2017)
Dust Indicators and Records from Terrestrial and Marine Palaeoenvironments (DIRTMAP)* ( <a href="https://www.lancaster.ac.uk/lec/sites/dirtmap/hw.html">https://www.lancaster.ac.uk/lec/sites/dirtmap/hw.html</a> )	$^{14}\text{C}$ and luminescence ages and other geochronological data.	Kohfeld and Harrison (2001); Mahar and Leedal (2014)
Radiocarbon Database (Delaware Geological Survey) ( <a href="https://www.dgs.udel.edu/datasets/">https://www.dgs.udel.edu/datasets/</a> )	$^{14}\text{C}$ ages.	Ramsey and Baxter (1996)
Canadian Archaeological Radiocarbon Database (CARD) ( <a href="https://www.canadianarchaeology.ca/">https://www.canadianarchaeology.ca/</a> )	$^{14}\text{C}$ ages.	Morlan (1999); Gajewski et al. (2011)
U.S. Geological Survey Science Base (ScienceBase Catalog Home)	All chronological data in any publication with a U.S. Geological Survey (USGS) author. These data are specifically tied to individual manuscripts but do include all metadata obtained from the USGS laboratories.	Gray et al. (2021) (example)

research theme, searchability, and perhaps most importantly, reporting standards. This latter problem deserves attention, because one of the main purposes of compiling luminescence data from studies worldwide into a centralized repository is to facilitate the comparison and evaluation of luminescence ages (Murray and Olley, 2002; Hesse, 2016; Neudorf et al., 2019a). Such data comparison and evaluation are only possible after careful consideration of the available independent age control, the methods of measurement and analysis used, and contributing sources of error.

## CONCLUSIONS

Luminescence methods provide a powerful lens into the age of deposits, Earth-surface processes and events, cultural material, sediment transport, and mineral characteristics. Given the diversity of applications and utilities, there is an even broader range of researchers publishing results and ultimately in need of access to data archives. However, the specialized nature of luminescence techniques and the multiple data components of the results necessitate a community-developed outline for publishing and archiving requirements that is similar to what has been developed for other geochronologic methods (Frankle et al., 2010; Fisher et al., 2014; Flowers et al., 2015; Horstwood et al., 2016;

Dutton et al., 2017). Involving the luminescence specialist early, and often, will help explain the reasoning behind the chronological science of luminescence dating.

Careful consideration of sample selection in relation to the target event of interest is critical to the successful application of luminescence dating. Target materials and sample sites should be selected to maximize the likelihood of complete bleaching (resetting) of the luminescence signal (sufficient exposure to light or heat). Collection of the sample in the field begins with consideration of the appropriate luminescence technique, age range of deposits or event to be dated, grain size of materials, mineral content, influence of site disturbance, environmental radioactivity, and luminescence characteristics of the target mineral.

Expecting a slow turnaround of data from the laboratory will help researchers avoid scheduling deadlines that are unrealistic. Instrumentation time is at a premium in laboratories, and the accumulated data needed to compile the  $D_E$  for a sample can take weeks. Many laboratories can only produce 50 or so ages a year per luminescence reader. If the sample is older (ca. >50 ka) it will require even more time on the machine because of the need to replicate the high burial dose and produce multiple steps and repeat points on a dose response curve. Several new advances can speed up the screening process,

including portable luminescence and standardized growth curve production, but ultimately a rigorous protocol completed on numerous aliquots is needed to obtain a reliable age.

While the age of the sample is key, there are characteristics of the generated  $D_E$  and  $D_R$  data that should be published with the resultant age. It is common to include one or two data-rich tables in papers presenting luminescence data (see Table 3).  $D_R$  information commonly includes elemental concentrations of K, U, and Th, cosmic dose rate, and moisture content values for each sample. The table also includes  $D_E$  data, the number of aliquots or grains analyzed to calculate the  $D_E$ , the scatter of the data, the age model used to extract the  $D_E$ —especially in complex environments—and finally the age. Luminescence ages are reported at  $1\sigma$  relative standard error, and the datum is based on the year of sample collection and never provided in yr B.P., which is exclusively reserved for radiocarbon dating.

This paper provides a review of commonly used luminescence dating methods and outlines publication and data reporting guidelines. Implementation of standardized reporting criteria will help authors, reviewers, editors, and readers assess the nuances of the luminescence data reported in a paper and identify key parts that are missing. Consistency in publications and data reporting will help streamline the publication

review process and improve data comparison among laboratories. Transferable data reporting styles and metadata content and format will also help with the development of data archives and allow greater utility of open-access databases. The sharing of data among research centers and scientific disciplines will advance knowledge and promote discovery across the geosciences.

## ACKNOWLEDGMENTS

During this time of pandemic, we are grateful for the time and resources given by many of our co-authors. We are especially thankful for those who gave when they were stretched as well as stressed by academic and research commitments. Reviews of previous versions of this paper by Harrison Gray and two anonymous reviewers helped to provide structure and rigor. This project was funded under both the Climate Research and the Federal Map Programs (Core Operations) of the U.S. Geological Survey and separately by Utah State University. G. Guérin received funding from the European Research Council (ERC) under the European Union's Horizon 2020 Research and Innovation Program (851793) Project Quina-World (ERC-StG-2019). Christina M. Neudorf was supported by the NSF Laboratory Technician Support grant 1914566. Any use of trade, firm, or product names is for descriptive purposes only and does not imply endorsement by the U.S. government.

## REFERENCES CITED

- Aitken, M.J., 1985, Thermoluminescence dating: Geochronology, v. 2, no. 1, <https://doi.org/10.1002/gea.3340020110>.
- Aitken, M.J., 1989, Luminescence dating: A guide for non-specialists: Archaeometry, v. 31, no. 2, p. 147–159, <https://doi.org/10.1111/j.1475-4754.1989.tb01010.x>.
- Aitken, M.J., 1998, An Introduction to Optical Dating: The Dating of Quaternary Sediments by the Use of Photon-Stimulated Luminescence: Oxford, UK, Oxford University Press, 267 p.
- Aitken, M.J., Tite, M.S., and Reid, J., 1964, Thermoluminescent dating of ancient ceramics: Nature, v. 202, p. 1032–1033, <https://doi.org/10.1038/2021032b0>.
- Aitken, M.J., and Valladas, H., 2014, Luminescence dating relevant to human origins, in Aitken, M.J., Stringer, C.B., and Mellars, P.A., eds., The Origin of Modern Humans and the Impact of Chronometric Dating: Princeton, New Jersey, Princeton University Press, p. 27–39.
- Ancient TL, 2017, Establishment of an international academic society for trapped charge dating: <http://ancienttl.org/SLED/SLED.htm> (accessed May 2021).
- Ankjaergaard, C., and Murray, A.S., 2007, Total beta and gamma dose rates in trapped charge dating based on beta counting: Radiation Measurements, v. 42, no. 3, p. 352–359, <https://doi.org/10.1016/j.radmeas.2006.12.007>.
- Ankjaergaard, C., Jain, M., and Wallinga, J., 2013, Towards dating Quaternary sediments using the quartz Violet Stimulated Luminescence (VSL) signal: Quaternary Geochronology, v. 18, p. 99–109, <https://doi.org/10.1016/j.quageo.2013.06.001>.
- Araújo, A.G., Feathers, J.K., Hartmann, G.A., Ladeira, F.S., Valezi, E.V., Nascimento, D.L., Ricci, O., de Oliveira Marum, V.J., and Ferreira da Trindade, R.I., 2020, Revisiting Alice Boer: Site formation processes and dating issues of a supposedly pre-Clovis site in Southeastern Brazil: Geoarchaeology, v. 2021, p. 1–27, <https://doi.org/10.1002/gea.21831>.
- Arnold, L., Demuro, M., Parés, J.M., Pérez-González, A., Arsuaga, J.L., Castro, J.M.B., and Carbonell, E., 2015, Evaluating the suitability of extended-range luminescence dating techniques over early and Middle Pleistocene timescales: Published datasets and case studies from Atapuerca, Spain: Quaternary International, v. 389, p. 167–190, <https://doi.org/10.1016/j.quaint.2014.08.010>.
- Arnold, L.J., and Roberts, R.G., 2009, Stochastic modelling of multi-grain equivalent dose (De) distributions: Implications for OSL dating of sediment mixtures: Quaternary Geochronology, v. 4, p. 204–230, <https://doi.org/10.1016/j.quageo.2008.12.001>.
- Arnold, L.J., Demuro, M., and Ruiz, M.N., 2012, Empirical insights into multi-grain averaging effects from 'pseudo' single-grain OSL measurements: Radiation Measurements, v. 47, no. 9, p. 652–658, <https://doi.org/10.1016/j.radmeas.2012.02.005>.
- Ashley, G.M., Ndiema, E.K., Spencer, J.Q.G., Harris, J.W.K., Kiura, P.W., Dibble, L., Du, A., and Lordan, P.T., 2017, Paleoenvironmental reconstruction of Dongodien, Lake Turkana, Kenya and OSL dating of site occupation during late Holocene climate change: African Archaeological Review, v. 34, p. 345–362, <https://doi.org/10.1007/s10437-017-9260-4>.
- Aubry, M.P., Van Couvering, J.A., Christie-Blick, N., Landing, E., Pratt, B.R., Owen, D.E., and Ferrusquia-Villafraña, I., 2009, Terminology of geological time: Establishment of a community standard: Stratigraphy, v. 6, no. 2, p. 100–105.
- Auclair, M., Lamothe, M., and Huot, S., 2003, Measurement of anomalous fading for feldspar IRSL using SAR: Radiation Measurements, v. 37, p. 487–492, [https://doi.org/10.1016/S1350-4487\(03\)00018-0](https://doi.org/10.1016/S1350-4487(03)00018-0).
- Bailey, R.M., 2010, Direct measurement of the fast component of quartz optically stimulated luminescence and implications for the accuracy of optical dating: Quaternary Geochronology, v. 5, no. 5, p. 559–568, <https://doi.org/10.1016/j.quageo.2009.10.003>.
- Bailey, R.M., and Arnold, L.J., 2006, Statistical modelling of single grain quartz De distributions and an assessment of procedures for estimating burial dose: Quaternary Science Reviews, v. 25, no. 19–20, p. 2475–2502, <https://doi.org/10.1016/j.quascirev.2005.09.012>.
- Ballarín, M., Wallinga, J., Wintle, A.G., and Bos, A.J.J., 2007, A modified SAR protocol for optical dating of individual grains from young quartz samples: Radiation Measurements, v. 42, p. 360–369, <https://doi.org/10.1016/j.radmeas.2006.12.016>.
- Bateman, M.D., 2015, The application of luminescence dating in sea-level studies, in Shennan, I., Long, A.L., and Horton, B.P., eds., Handbook of Sea-Level Research: Wiley Online Books, p. 404–417.
- Bateman, M.D., 2019, Sampling to reporting in Bateman, M.D., ed., Handbook of Luminescence Dating: Scotland, UK, Whittles Publishing, p. 40–61.
- Bateman, M.D., Frederick, C.D., Jaiswal, M.K., and Singhvi, A.K., 2003, Investigations into the potential effects of pedoturbation on luminescence dating: Quaternary Science Reviews, v. 22, no. 10–13, p. 1169–1176, [https://doi.org/10.1016/S0277-3791\(03\)00019-2](https://doi.org/10.1016/S0277-3791(03)00019-2).
- Berger, G.W., Almond, P.C., and Pillans, B.J., 2001, Luminescence dating and glacial stratigraphy in Westland, New Zealand: New Zealand Journal of Geology and Geophysics, v. 44, no. 1, p. 25–35, <https://doi.org/10.1080/00288306.2001.9514919>.
- Blong, R.J., and Gillespie, R., 1978, Fluvially transported charcoal gives erroneous <sup>14</sup>C ages for recent deposits: Nature, v. 271, p. 739–741, <https://doi.org/10.1038/271739a0>.
- Bøtter-Jensen, L., Bulur, E., Duller, G.A.T., and Murray, A.S., 2000, Advances in luminescence instruments: Radiation Measurements, v. 32, p. 523–528, [https://doi.org/10.1016/S1350-4487\(00\)00039-1](https://doi.org/10.1016/S1350-4487(00)00039-1).
- Bøtter-Jensen, L., Thomsen, K.J., and Jain, M., 2010, Review of optically stimulated luminescence (OSL): Instrumental developments for retrospective dosimetry: Radiation Measurements, v. 45, no. 3–6, p. 253–257, <https://doi.org/10.1016/j.radmeas.2009.11.030>.
- Box, G.E.P., 1976, Science and statistics: Journal of the American Statistical Association, v. 71, no. 356, p. 791–799, <https://doi.org/10.1080/01621459.1976.10480949>.
- Broecker, W.S., and Walton, A., 1959, Radiocarbon from nuclear tests: Science, v. 130, p. 309–314, <https://doi.org/10.1126/science.130.3371.309>.
- Brown, J.W., Feathers, J.K., Chatters, J.C., McCutcheon, P.T., and Hackenberger, S., 2018, Chronometric precision and accuracy: Radiocarbon and luminescence age estimates for Pacific Northwest cooking features: Canadian Journal of Archaeology, v. 42, p. 240–254.
- Brown, N.D., 2020, Which geomorphic processes can be informed by luminescence measurements?: Geomorphology, v. 367, <https://doi.org/10.1016/j.geomorph.2020.107296>.
- Buckland, P.I., 2014, SEAD—The strategic environmental archaeology database. Inter-linking multiproxy environmental data with archaeological investigations and ecology: CAA2012, in Proceedings, 40th Conference in Computer Applications and Quantitative Methods in Archaeology, Southampton, UK, p. 320–330, <https://doi.org/10.13140/RG.2.1.2512.1042>.
- Bulur, E., Bøtter-Jensen, L., and Murray, A.S., 2000, Optically stimulated luminescence from quartz measured using the linear modulation technique: Radiation Measurements, v. 32, no. 5–6, p. 407–411, [https://doi.org/10.1016/S1350-4487\(00\)00115-3](https://doi.org/10.1016/S1350-4487(00)00115-3).
- Burow, C., 2020, calc\_CosmicDoseRate(): Calculate the cosmic dose rate. Function version 0.5.2, in Kreutzer, S., Burow, C., Dietze, M., Fuchs, M.C., Schmidt, C., Fischer, M., Friedrich, J., Riedesel, S., Autzen, M., and Mittelstrass, D., 2020, Luminescence: Comprehensive Luminescence Dating Data Analysis. R package version 0.9.10, <https://CRAN.R-project.org/package=Luminescence>.
- Burrow, S., 2017, Radiocarbon analysis in Wales: The state of the nation: Archaeology in Wales, v. 56, p. 107–112.
- Buylaert, J.P., Murray, A.S., Thomsen, K.J., and Jain, M., 2009, Testing the potential of an elevated temperature IRSL signal from K-feldspar: Radiation Measurements, v. 44, p. 560–565, <https://doi.org/10.1016/j.radmeas.2009.02.007>.
- Buylaert, J.P., Jain, M., Murray, A.S., Thomsen, K.J., Theil, C., and Sohbati, R., 2012, A robust feldspar luminescence dating method for Middle and Late Pleistocene sediments: Boreas, v. 41, p. 435–451, <https://doi.org/10.1111/j.1502-3885.2012.00248.x>.
- Chapot, M.S., Sohbati, R., Murray, A.S., Pederson, J.L., and Rittenour, T.M., 2012, Constraining the age of rock art by dating a rockfall event using sediment and rock-surface luminescence dating techniques: Quaternary Geochronology, v. 13, p. 18–25, <https://doi.org/10.1016/j.quageo.2012.08.005>.
- Codilean, A.T., Munack, H., Cohen, T.J., Saktura, W.M., Gray, A., and Mudd, S.M., 2018, OCTOPUS: An open cosmogenic isotope and luminescence database: Earth System Science Data, v. 10, p. 2123–2139, <https://doi.org/10.5194/essd-10-2123-2018>.
- Combès, B., and Philippe, A., 2017, Bayesian analysis of individual and systematic multiplicative errors for estimating ages with stratigraphic constraints in optically stimulated luminescence dating: Quaternary Geochronology, v. 39, p. 24–34, <https://doi.org/10.1016/j.quageo.2017.02.003>.
- Cunningham, A.C., and Wallinga, J., 2010, Selection of integration time intervals for quartz OSL decay curves: Quaternary Geochronology, v. 5, p. 657–666, <https://doi.org/10.1016/j.quageo.2010.08.004>.
- Cunningham, A.C., Evans, M., and Knight, J., 2015, Quantifying bleaching for zero-age fluvial sediment: A Bayesian Approach: Radiation Measurements, v. 81, p. 55–61, <https://doi.org/10.1016/j.radmeas.2015.04.007>.
- Davids, F., Wallinga, J., Johns, C.A., and Partners, N.C.L., 2006, LumiD: The NCL luminescence database: NCL Symposium Series, v. 4, p. 2–3.
- del Río, I., Sawakuchi, A.O., and González, G., 2019, Luminescence dating of sediments from central Atacama Desert, northern Chile: Quaternary Geochronology, v. 53, 101002, <https://doi.org/10.1016/j.quageo.2019.05.001>.
- Demuro, M., Roberts, R.G., Froese, D.G., Arnold, L.J., Brock, F., and Ramsey, C.B., 2008, Optically stimulated luminescence dating of single and multiple grains of quartz from perennially frozen loess in western Yukon Territory, Canada: Comparison with radiocarbon chronologies for the late Pleistocene Dawson tephra: Quaternary Geochronology, v. 3, no. 4, p. 346–364, <https://doi.org/10.1016/j.quageo.2007.12.003>.
- Denby, P.M., Bøtter-Jensen, L., Murray, A.S., Thomsen, K.J., and Moska, P., 2006, Application of pulsed OSL to the



- separation of the luminescence components from a mixed quartz/feldspar sample: Radiation Measurements, v. 41, no. 7–8, p. 774–779, <https://doi.org/10.1016/j.radmeas.2006.05.017>.
- DeWitt, R., McKeever, S., Lamothe, M., Huot, S., Bell, A., Vila, M., and Zacny, K., 2012, A Mars in-situ luminescence reader for geochronology, mineral identification, and radiation measurements: International Workshop on Instrumentation for Planetary Missions, Lunar and Planetary Institute 1019, <https://www.lpi.usra.edu/meetings/ipm2012/pdf/1019.pdf>.
- Dietze, M., Kreutzer, S., Burow, C., Fuchs, M.C., Fischer, M., and Schmidt, C., 2016, The abanico plot: Visualizing chronometric data with individual standard errors: Quaternary Geochronology, v. 31, p. 12–18, <https://doi.org/10.1016/j.quageo.2015.09.003>.
- Duller, G.A.T., 1991, Equivalent dose determination using single aliquots: Nuclear Tracks and Radiation Measurements, v. 18, p. 371–378.
- Duller, G.A.T., 2004, Luminescence dating of Quaternary sediments: Recent advances: Journal of Quaternary Science, v. 19, p. 183–192, <https://doi.org/10.1002/jqs.809>.
- Duller, G.A.T., 2008a, Luminescence Dating: Guidelines on Using Luminescence Dating in Archaeology: Swindon, UK, English Heritage, 44 p.
- Duller, G.A.T., 2008b, Single-grain optical dating of Quaternary sediments: Why aliquot size matters in luminescence dating: Boreas, v. 37, no. 4, p. 589–612, <https://doi.org/10.1111/j.1502-3885.2008.00051.x>.
- Duller, G.A.T., 1991, Equivalent dose determination using single aliquots: International Journal of Radiation Applications and Instrumentation Part D: Nuclear Tracks and Radiation Measurements, v. 18, no. 4, p. 371–378, [https://doi.org/10.1016/1359-0189\(91\)90002-Y](https://doi.org/10.1016/1359-0189(91)90002-Y).
- Duller, G.A.T., Bøtter-Jensen, L., Murray, A.S., and Truscott, A.J., 1999, Single grain laser luminescence (SGLL) measurements using a novel automated reader: Nuclear Instruments & Methods in Physics Research Section B: Beam Interactions with Materials and Atoms, v. 155, no. 4, p. 506–514, [https://doi.org/10.1016/S0168-583X\(99\)00488-7](https://doi.org/10.1016/S0168-583X(99)00488-7).
- Duller, G.A.T., Bøtter-Jensen, L., and Murray, A.S., 2000, Optical dating of single sand-sized grains of quartz: Sources of variability: Radiation Measurements, v. 32, no. 5–6, p. 453–457, [https://doi.org/10.1016/S1350-4487\(00\)00055-X](https://doi.org/10.1016/S1350-4487(00)00055-X).
- Duller, G.A.T., Penkman, K.E.H., and Wintle, A.G., 2009, Assessing the potential for using biogenic calcites as dosimeters for luminescence dating: Radiation Measurements, v. 44, no. 5–6, p. 429–433, <https://doi.org/10.1016/j.radmeas.2009.02.008>.
- Durcan, J.A., and Duller, G.A.T., 2011, The fast ratio: A rapid measure for testing the dominance of the fast component in the initial OSL signal from quartz: Radiation Measurements, v. 46, p. 1065–1072, <https://doi.org/10.1016/j.radmeas.2011.07.016>.
- Durcan, J.A., King, G.E., and Duller, G.A.T., 2015, DRAC: Dose rate and age calculator for trapped charge dating: Quaternary Geochronology, v. 28, p. 54–61, <https://doi.org/10.1016/j.quageo.2015.03.012>.
- DuRoss, C.B., Gold, R.D., Gray, H.J., and Nicovich, S.R., 2022, Portable optically stimulated luminescence age map of a paleoseismic exposure: Geology, v. 50, p. 470–475, <https://doi.org/10.1130/G49472.1>.
- Dutton, A., Rubin, K., McLean, N., Bowring, J., Bard, E., Edwards, R.L., Henderson, G.M., Reid, M.R., Richards, D.A., Sims, K.W.W., and Walker, J.D., 2017, Data reporting standards for publication of U-series data for geochronology and timescale assessment in the earth sciences: Quaternary Geochronology, v. 39, p. 142–149, <https://doi.org/10.1016/j.quageo.2017.03.001>.
- Ellerton, D., Rittenour, T., Shulmeister, J., Gontz, A., Welsh, K.J., and Patton, N., 2020, An 800 kyr record of dune emplacement in relationship to high sea level forcing, Coolool Sand Mass, Queensland, Australia: Geomorphology, v. 354, <https://doi.org/10.1016/j.geomorph.2019.106999>.
- Fattahi, M., and Stokes, S., 2000, Extending the time range of luminescence dating using red TL (RTL) from volcanic quartz: Radiation Measurements, v. 32, no. 5, p. 479–485, [https://doi.org/10.1016/S1350-4487\(00\)00105-0](https://doi.org/10.1016/S1350-4487(00)00105-0).
- Feathers, J.K., 2003, Use of luminescence dating in archaeology: Measurement Science & Technology, v. 14, p. 1493–1509, <https://doi.org/10.1088/0957-0233/14/9/302>.
- Feathers, J.K., 2009, Problems of ceramic chronology in the Southeast: Does shell-tempered pottery appear earlier than we think? American Antiquity, v. 74, p. 113–142, <https://doi.org/10.1017/S0002731600047533>.
- Feathers, J.K., and Rhode, D., 1998, Luminescence dating of protohistoric pottery from the Great Basin: Geoarchaeology, v. 13, no. 3, p. 287–308, [https://doi.org/10.1002/\(SICI\)1520-6548\(199802\)13:3<287::AID-GEA3>3.0.CO;2-0](https://doi.org/10.1002/(SICI)1520-6548(199802)13:3<287::AID-GEA3>3.0.CO;2-0).
- Feathers, J.K., and Tunnicliffe, J., 2011, Effect of single-grain versus multi-grain aliquots in determining age for K-feldspars from southwestern British Columbia: Ancient TL, v. 29, p. 53–58.
- Feathers, J.K., Zedeño, M.N., Todd, L.C., and Aaberg, S., 2015, Dating stone alignments by luminescence: Advances in Archaeological Practice, v. 3, no. 4, p. 378–396, <https://doi.org/10.7183/2326-3768.3.4.378>.
- Feathers, J., Evans, M., Stratford, D., and de la Peña, P., 2020, Exploring complexity in luminescence dating of quartz and feldspars at the Middle Stone Age site of Mbulu's cave (Limpopo, South Africa): Quaternary Geochronology, v. 59, <https://doi.org/10.1016/j.quageo.2020.101092>.
- Fenn, K., Durcan, J.A., Thomas, D.S., Millar, I.L., and Marković, S.B., 2020, Re-analysis of Late Quaternary dust mass accumulation rates in Serbia using new luminescence chronology for loess-paleosol sequence at Surduk: Boreas, v. 49, no. 3, p. 634–652, <https://doi.org/10.1111/bor.12445>.
- Fisher, C.M., Vervoort, J.D., and Hanchar, J.M., 2014, Guidelines for reporting zircon Hf isotopic data by LA-MC-ICPMS and potential pitfalls in the interpretation of these data: Chemical Geology, v. 363, p. 125–133, <https://doi.org/10.1016/j.chemgeo.2013.10.019>.
- Flowers, R.M., Farley, K.A., and Ketcham, R.A., 2015, A reporting protocol for thermochronologic modeling illustrated with data from the Grand Canyon: Earth and Planetary Science Letters, v. 432, p. 425–435, <https://doi.org/10.1016/j.epsl.2015.09.053>.
- Frankel, K.L., Finkel, R.C., and Owen, L.A., 2010, Terrestrial Cosmogenic Nuclide Geochronology Data Reporting Standards Needed: Eos (Washington, D.C.), v. 91, <https://doi.org/10.1029/2010EO040003>.
- Frouin, M., Guérin, G., Lahaye, C., Mercier, N., Huot, S., Aldeias, V., Bruxelles, L., Chiotti, L., Dibble, H.L., Goldberg, P., Madelaine, S., McPherron, S.J.P., Sandgathe, D., Steele, T.E., and Turq, A., 2017a, New luminescence dating results based on polymineral fine grains from the Middle and Upper Palaeolithic site of La Ferrassie (Dordogne, SW France): Quaternary Geochronology, v. 39, p. 131–141, <https://doi.org/10.1016/j.quageo.2017.02.009>.
- Frouin, M., Huot, S., Kreutzer, S., Lahaye, C., Lamothe, M., Philippe, A., and Mercier, N., 2017b, An improved radiofluorescence single-aliquot regenerative dose protocol for K-feldspars: Quaternary Geochronology, v. 38, p. 13–24, <https://doi.org/10.1016/j.quageo.2016.11.004>.
- Fuchs, M., and Lang, A., 2009, Luminescence dating of hillslope deposits—A review: Geomorphology, v. 109, p. 17–26, <https://doi.org/10.1016/j.geomorph.2008.08.025>.
- Gajewski, K., Munoz, S., Peros, M., Viau, A., Morlan, R., and Betts, M., 2011, The Canadian Archaeological Radiocarbon Database (CARD): Archaeological <sup>14</sup>C dates in North America and their paleoenvironmental context: Radiocarbon, v. 53, no. 2, p. 371–394, <https://doi.org/10.1017/S0033822200056630>.
- Galbraith, R.F., 1990, The radial plot: Graphical assessment of spread in ages: International Journal of Radiation Applications and Instrumentation. Part D: Nuclear Tracks and Radiation Measurements, v. 17, no. 3, p. 207–214, [https://doi.org/10.1016/1359-0189\(90\)90036-W](https://doi.org/10.1016/1359-0189(90)90036-W).
- Galbraith, R.F., 2005, Statistics for Fission Track Analysis: Boca Raton, Florida, Chapman & Hall/CRC Press, 240 p., <https://doi.org/10.1201/9781420034929>.
- Galbraith, R.F., and Roberts, R.G., 2012, Statistical aspects of equivalent dose and error calculation and display in OSL dating: An overview and some recommendations: Quaternary Geochronology, v. 11, p. 1–27, <https://doi.org/10.1016/j.quageo.2012.04.020>.
- Galbraith, R.F., Roberts, R.G., Laslett, G.M., Yoshida, H., and Olley, J.M., 1999, Optical dating of single and multiple grains of quartz from Jinnium rock shelter, northern Australia: Part I, experimental design and statistical models: Archaeometry, v. 41, no. 2, p. 339–364, <https://doi.org/10.1111/j.1475-4754.1999.tb00987.x>.
- Gagez, C., and Mercier, N., 2012, Anatol software (Analyse Thermo Opto Luminescence).
- Glignic, L.A., May, J.H., and Cohen, T.J., 2015, All mixed up: Using single-grain equivalent dose distributions to identify phases of pedogenic mixing on a dryland alluvial fan: Quaternary International, v. 362, p. 23–33, <https://doi.org/10.1016/j.quaint.2014.07.040>.
- Glignic, L.A., Cohen, T.J., Slack, M., and Feathers, J.K., 2016, Sediment mixing in aeolian sandsheets identified and quantified using single-grain optically stimulated luminescence: Quaternary Geochronology, v. 32, p. 53–66, <https://doi.org/10.1016/j.quageo.2015.12.006>.
- Gray, H.J., Mahan, S.A., Rittenour, T.M., and Nelson, M.S., 2015, Guide to luminescence dating techniques and their application for paleoseismic research, in Lund, W.R., ed., Proceedings, Basin and Range Province Seismic Hazards Summit III: Utah Geological Survey and Western States Seismic Policy Council, 18 p.
- Gray, H.J., Tucker, G.E., Mahan, S.A., McGuire, C., and Rhodes, E.J., 2017, On extracting sediment transport information from measurements of luminescence in river sediment: Journal of Geophysical Research: Earth Surface, v. 122, no. 3, p. 654–677, <https://doi.org/10.1002/2016JF003858>.
- Gray, H.J., Mahan, S.A., Springer, K.B., and Pigati, J.S., 2018, Examining the relationship between portable luminescence reader measurements and depositional ages of paleowetland sediments, Las Vegas Valley, Nevada: Quaternary Geochronology, v. 48, p. 80–90, <https://doi.org/10.1016/j.quageo.2018.07.006>.
- Gray, H.J., Jain, M., Sawakuchi, A.O., Mahan, S.A., and Tucker, G.E., 2019, Luminescence as a sediment tracer and provenance tool: Reviews of Geophysics, v. 57, p. 987–1017, <https://doi.org/10.1029/2019RG000646>.
- Gray, H.J., Keen-Zebert, A., Furbish, D.J., Tucker, G.E., and Mahan, S.A., 2020, Depth-dependent soil mixing persists across climate zones: Proceedings of the National Academy of Sciences of the United States of America, v. 117, p. 8750–8756, <https://doi.org/10.1073/pnas.1914101117>.
- Gray, H.J., DuRoss, C.B., Gold, R.D., and Nicovich, S.R., 2021, Geochronological data for the Deep Creek paleoseismic site, Wasatch fault zone, Utah: U.S. Geological Survey Data Release, <https://doi.org/10.5066/P9YX88LK>.
- Groza-Săcaci, S.M., Panaiotu, C., and Timar-Gabor, A., 2020, Single aliquot regeneration (SAR) optically stimulated luminescence dating protocols using different grain-sizes of quartz: Revisiting the chronology of Mircea Vodă loess-paleosol master section (Romania): Methods and Protocols, v. 3, no. 1, 19 p., <https://doi.org/10.3390/mps3010019>.
- Grün, R., 2009, The DATA program for the calculation of ESR age estimates on tooth enamel: Quaternary Geochronology, v. 4, p. 231–232, <https://doi.org/10.1016/j.quageo.2008.12.005>.
- Guedes, C.C.F., Giannini, P.C.F., Sawakuchi, A.O., DeWitt, R., and Aguiar, V.P.A., 2017, Weakening of northeast trade winds during the Heinrich stadial 1 event recorded by dune field stabilization in tropical Brazil: Quaternary Research, v. 88, p. 369–381, <https://doi.org/10.1017/jqua.2017.79>.
- Guérin, G., Mercier, N., Nathan, R., Adamiec, G., and LeFrais, Y., 2012, On the use of the infinite matrix assumption and associated concepts: A critical review: Radiation Measurements, v. 47, p. 778–785, <https://doi.org/10.1016/j.radmeas.2012.04.004>.
- Guérin, G., Murray, A.S., Jain, M., Thomsen, K.J., and Mercier, N., 2013, How confident are we in the chronology of the transition between Howieson's Poort and Still Bay: Journal of Human Evolution, v. 64, no. 4, p. 314–317, <https://doi.org/10.1016/j.jhevol.2013.01.006>.
- Guérin, G., Frouin, M., Talamo, S., Aldeias, V., Bruxelles, L., Chiotti, L., Dibble, H.L., Goldberg, P., Hublin, J.-J., Jain, M., Lahaye, C., Madelaine, S., Maureille, B., McPherron, S.J.P., Mercier, N., Murray, A.S., Sandgathe, D., Steele, T.E., Thomsen, K., and Turq, A., 2015, A multi-method luminescence dating of the Palaeolithic sequence of La Ferrassie based on new excavations adjacent to the La Ferrassie 1 and 2 skeletons:

- Journal of Archaeological Science, v. 58, p. 147–166, <https://doi.org/10.1016/j.jas.2015.01.019>.
- Guérin, G., Christophe, C., Philippe, A., Murray, A.S., Thomsen, K.J., Tribolo, C., Urbanova, P., Jain, M., Guibert, P., Mercier, N., Kreutzer, S., and Lahaye, C., 2017, Absorbed dose, equivalent dose, measured dose rates, and implications for OSL age estimates: Introducing the average dose model: Quaternary Geochronology, v. 41, p. 163–173, <https://doi.org/10.1016/j.quageo.2017.04.002>.
- Guérin, G., Lahaye, C., Heydari, M., Autzen, M., Buylaert, J.P., Guibert, P., Jain, M., Kreutzer, S., Lebrun, B., Murray, A.S., Thomsen, K.J., Urbanova, P., and Philippe, A., 2021, Towards an improvement of OSL age uncertainties: Modelling OSL ages with systematic errors, stratigraphic constraints and radiocarbon ages using the R package BayLum: Geochronology, v. 3, p. 229–245, <https://doi.org/10.5194/gchron-3-229-2021>.
- Guralnik, B., Jain, M., Herman, F., Paris, R.B., Harrison, T.M., Murray, A.S., Valla, P.G., and Rhodes, E.J., 2013, Effective closure temperature in leaky and/or saturating thermochronometers: Earth and Planetary Science Letters, v. 384, p. 209–218, <https://doi.org/10.1016/j.epsl.2013.10.003>.
- Guralnik, B., Jain, M., Herman, F., Ankjærgaard, C., Murray, A.S., Valla, P.G., Preusser, F., King, G.E., Chen, R., Lowick, S.E., and Kook, M., 2015, OSL-thermochronometry of feldspar from the KTB borehole, Germany: Earth and Planetary Science Letters, v. 423, p. 232–243, <https://doi.org/10.1016/j.epsl.2015.04.032>.
- Harrison, T.M., Baldwin, S.L., Caffee, M., Gehrels, G.E., Schoene, B., Shuster, D.L., and Singer, B.S., 2015, It's about time: Opportunities and challenges for US geochronology: Institute of Geophysics and Planetary Physics Publication 6539, 56 p.
- Heaton, T.J., Blaauw, M., Blackwell, P.G., Bronk Ramsey, C., Reimer, P.J., and Scott, E.M., 2020, The IntCal20 approach to radiocarbon calibration curve construction: A new methodology using Bayesian splines and errors-in-variables: Radiocarbon, v. 62, no. 4, p. 821–863, <https://doi.org/10.1017/RDC.2020.46>.
- Hesse, P.P., 2016, How do longitudinal dunes respond to climate forcing? Insights from 25 years of luminescence dating of the Australian desert dunefields: Quaternary International, v. 410, p. 11–29, <https://doi.org/10.1016/j.quaint.2014.02.020>.
- Heydari, M., and Guérin, G., 2018, OSL signal saturation and dose rate variability: Investigating the behaviour of different statistical models: Radiation Measurements, v. 120, p. 96–103, <https://doi.org/10.1016/j.radmeas.2018.05.005>.
- Horstwood, M.S., Köhler, J., Gehrels, G., Jackson, S.E., McLean, N.M., Paton, C., Pearson, N.J., Sircombe, K., Sylvester, P., Vermeesch, P., and Bowring, J.F., 2016, Community-derived standards for LA-ICP-MS U-(Th)-Pb geochronology—Uncertainty propagation, age interpretation and data reporting: Geostandards and Geoanalytical Research, v. 40, no. 3, p. 311–332, <https://doi.org/10.1111/j.1751-908X.2016.00379.x>.
- Hu, Y., Li, B., and Jacobs, Z., 2020, Single-grain quartz OSL characteristics: Testing for correlations within and between sites in Asia, Europe and Africa: Methods and Protocols, v. 3, 3888092, <https://doi.org/10.3390/mps3010002>.
- Huntley, D.J., and Lamothe, M., 2001, Ubiquity of anomalous fading in K-feldspars and the measurement and correction for it in optical dating: Canadian Journal of Earth Sciences, v. 38, p. 1093–1106, <https://doi.org/10.1139/e01-013>.
- Huntley, D.J., Godfrey-Smith, D.I., and Thewalt, M.L.W., 1985, Optical dating of sediments: Nature, v. 313, p. 105–107.
- Ideker, C.J., Finley, J.B., Rittenour, T.M., and Nelson, M.S., 2017, Single-grain optically stimulated luminescence dating of quartz temper from prehistoric Intermountain Ware ceramics, northwestern Wyoming, USA: Quaternary Geochronology, v. 42, p. 42–55, <https://doi.org/10.1016/j.quageo.2017.07.004>.
- Lancaster, N., Wolfe, S., Thomas, D., Bristow, C., Bubenzer, O., Burrough, S., Duller, G., Halfen, A., Hesse, P., Roskiny, J., Singhvi, A., Tsor, H., Tripaldi, A., Yang, X., and Zárte, M., 2016, The INQUA Dunes Atlas chronologic database: Quaternary International, v. 410, no. B, p. 3–10, <https://doi.org/10.1016/j.quaint.2015.10.044>.
- IPCC (Shukla, P.R., Skea, J., Calvo Buendia, E., Masson-Delmotte, V., Pörtner, H.-O., Roberts, D. C., Zhai, P., Slade, R., Connors, S., van Diemen, R., Ferrat, M., Haughey, E., Luz, S., Neogi, S., Pathak, M., Petzold, J., Portugal Pereira, J., Vyas, P., Huntley, E., Kissick, K., Belkacemi, M., and Malley, J., eds.), 2019, Climate Change and Land: An IPCC Special Report on Climate Change, Desertification, Land Degradation, Sustainable Land Management, Food Security, and Greenhouse Gas Fluxes in Terrestrial Ecosystems, 874 p., <https://www.ipcc.ch/site/assets/uploads/2019/11/SRCL-Full-Report-Compiled-191128.pdf>.
- Jain, M., 2009, Extending the dose range: Probing deep traps in quartz with 3.06 eV photons: Radiation Measurements, v. 44, no. 5–6, p. 445–452, <https://doi.org/10.1016/j.radmeas.2009.03.011>.
- Jain, M., Murray, A.S., and Bøtter-Jensen, L., 2004, Optically stimulated luminescence dating: How significant is incomplete light exposure in fluvial environments? Datation par luminescence stimulée optiquement: quelle signification en cas de blanchiment incomplet des sédiments fluviaux? Quaternaire, v. 15, no. 1, p. 143–157, <https://doi.org/10.3406/quate.2004.1762>.
- Kars, R.H., and Wallinga, J., 2009, IRSL dating of K-feldspars: Modelling natural dose response curves to deal with anomalous fading and trap competition: Radiation Measurements, v. 44, no. 5–6, p. 594–599, <https://doi.org/10.1016/j.radmeas.2009.03.032>.
- Kars, R.H., Wallinga, J., and Cohen, K.M., 2008, A new approach towards anomalous fading correction for feldspar IRSL dating—tests on samples in field saturation: Radiation Measurements, v. 43, no. 2–6, p. 786–790, <https://doi.org/10.1016/j.radmeas.2008.01.021>.
- King, G.E., Guralnik, B., Valla, P.G., and Herman, F., 2016, Trapped-charge thermochronometry and thermometry: A status review: Chemical Geology, v. 446, p. 3–17, <https://doi.org/10.1016/j.chemgeo.2016.08.023>.
- King, G.E., Valla, P.G., and Lehmann, B., 2019, Rock surface burial and exposure dating, in Bateman, M.D., ed., Handbook of Luminescence Dating: Scotland, UK, Whittles Publishing, p. 350–393.
- Kohfeld, K.E., and Harrison, S.P., 2001, DIRTMAP: The geological record of dust: Earth-Science Reviews, v. 54, p. 81–114, [https://doi.org/10.1016/S0012-8252\(01\)00042-3](https://doi.org/10.1016/S0012-8252(01)00042-3).
- Kreutzer, S., Mauz, B., Martin, L., and Mercier, N., 2019, ‘RCarb’: Dose rate modelling of carbonate-rich samples—an implementation of carb in R: Ancient TL, v. 37, p. 1–8.
- Kreutzer, S., Dietze, M., and Burrow, C., 2020, use\_DRAC(): Use DRAC to calculate dose rate data. Function version 0.1.3, in Kreutzer, S., Burrow, C., Dietze, M., Fuchs, M.C., Schmidt, C., Fischer, M., Friedrich, J., Riedesel, S., Autzen, M., and Mittelstrass, D., Luminescence: Comprehensive Luminescence Dating Data Analysis: R package version 0.9.10, <https://cran.r-project.org/web/packages/Luminescence/Luminescence.pdf>.
- Kumar, R., Kook, M., and Jain, M., 2021, Sediment dating using infrared photoluminescence: Quaternary Geochronology, v. 62, <https://doi.org/10.1016/j.quageo.2020.101147>.
- Lai, Z., 2010, Chronology and the upper dating limit for loess samples from Luochuan section in the Chinese Loess Plateau using quartz OSL SAR protocol: Journal of Asian Earth Sciences, v. 37, no. 2, p. 176–185, <https://doi.org/10.1016/j.jseaes.2009.08.003>.
- Lamothe, M., Auclair, M., Hamzaoui, C., and Huot, S., 2003, Towards a prediction of long-term anomalous fading of feldspar IRSL: Radiation Measurements, v. 37, no. 4–5, p. 493–498, [https://doi.org/10.1016/S1350-4487\(03\)00016-7](https://doi.org/10.1016/S1350-4487(03)00016-7).
- Lamothe, M., Forget Brissou, L., and Hardy, F., 2020, Circumvention of anomalous fading in feldspar luminescence dating using Post-Isothermal IRSL: Quaternary Geochronology, v. 57, <https://doi.org/10.1016/j.quageo.2020.101062>.
- Lancaster, N., Wolfe, S., Thomas, D., Bristow, C., Bubenzer, O., Burrough, S., Duller, G., Halfen, A., Hesse, P., Roskiny, J., Singhvi, A., Tsor, H., Tripaldi, A., Yang, X., and Zárte, M., 2016, The INQUA Dunes Atlas chronologic database: Quaternary International, v. 410, no. B, p. 3–10, <https://doi.org/10.1016/j.quaint.2015.10.044>.
- Lapp, T., Jain, M., Ankjærgaard, C., and Pirtzel, L., 2009, Development of pulsed stimulation and Photon Timer attachments to the Risø TL/OSL reader: Radiation Measurements, v. 44, no. 5–6, p. 571–575, <https://doi.org/10.1016/j.radmeas.2009.01.012>.
- Larsson, C., Koslowsky, V., Gao, H., Khanna, S., and Estan, D., 2005, Optically stimulated luminescence in forensics: Applied Radiation and Isotopes, v. 63, no. 5–6, p. 689–695, <https://doi.org/10.1016/j.apradiso.2005.05.019>.
- Lawson, M.J., Roder, B.J., Stang, D.M., and Rhodes, E.J., 2012, OSL and IRSL characteristics of quartz and feldspar from southern California, USA: Radiation Measurements, v. 47, no. 9, p. 830–836, <https://doi.org/10.1016/j.radmeas.2012.03.025>.
- Li, B., and Li, S.-H., 2011, Luminescence dating of K-feldspar from sediments: A protocol without anomalous fading correction: Quaternary Geochronology, v. 6, p. 468–479, <https://doi.org/10.1016/j.quageo.2011.05.001>.
- Lian, O.B., and Roberts, R.G., 2006, Dating the Quaternary: Progress in luminescence dating of sediments: Quaternary Science Reviews, v. 25, p. 2449–2468, <https://doi.org/10.1016/j.quascirev.2005.11.013>.
- Liang, P., and Forman, S.L., 2019, LDAC: An Excel-based program for luminescence equivalent dose and burial age calculations: Ancient TL, v. 37, p. 21–40.
- Liritzis, I., Singhvi, A.K., Feathers, J.K., Wagner, G.A., Kaderit, A., Zacharias, N., and Li, S.-H., 2013, Luminescence Dating in Archaeology, Anthropology and Geoarchaeology: Berlin, Springer-Verlag, 70 p., <https://doi.org/10.1007/978-3-319-00170-8>.
- Liu, J., Cui, F., Murray, A.S., Sohbati, R., Jain, M., Gao, H., Li, W., Li, C., Li, P., Zhou, T., and Chen, J., 2019, Re-setting of the luminescence signal in modern riverbed cobbles along the course of the Shiyang River, China: Quaternary Geochronology, v. 49, p. 184–190, <https://doi.org/10.1016/j.quageo.2018.04.004>.
- Liu, T., Greenbaum, N., Baker, V.R., Ji, L., Onken, J., Weisheit, J., Porat, N., and Rittenour, T., 2020, Paleoflood hydrology on the lower Green River, upper Colorado River Basin, USA: An example of a naturalist approach to flood-risk analysis: Journal of Hydrology, v. 580, <https://doi.org/10.1016/j.jhydrol.2019.124337>.
- López, G.I., and Thompson, J.W., 2012, OSL and sediment accumulation rate models: Understanding the history of sediment deposition: Quaternary Geochronology, v. 10, p. 175–179, <https://doi.org/10.1016/j.quageo.2012.02.026>.
- López, G.I., Goodman-Tchernov, B.N., and Porat, N., 2018, OSL over-dispersion: A pilot study for the characterization of extreme events in the shallow marine realm: Sedimentary Geology, v. 378, p. 35–51, <https://doi.org/10.1016/j.sedgeo.2018.09.002>.
- Madsen, A.T., and Murray, A.S., 2009, Optically stimulated luminescence dating of young sediments: A review: Geomorphology, v. 109, no. 1–2, p. 3–16, <https://doi.org/10.1016/j.geomorph.2008.08.020>.
- Mahan, S., and Kay, J., 2012, Building on previous OSL dating techniques for gypsum: A case study from Salt Basin playa, New Mexico and Texas: Quaternary Geochronology, v. 10, p. 345–352, <https://doi.org/10.1016/j.quageo.2012.02.001>.
- Mahan, S.A., Donlan, R.A., and Kardos, B., 2015, Luminescence dating of anthropogenic features of the San Luis Valley, Colorado: From stone huts to stone walls: Quaternary International, v. 362, p. 50–62, <https://doi.org/10.1016/j.quaint.2014.09.067>.
- Mahan, S.A., and DeWitt, R.L., 2019, Principles and history of luminescence dating, Chapter 1 in Bateman, M., ed., Handbook of Luminescence Dating: Caithness, UK, Whittles Publishing, p. 1–39.
- Mahar, B.A., and Leedal, D.T., 2014, DIRTMAP: Development of a web-based dust archive: PAGES Magazine, v. 22, no. 2, 90 p.
- Martin, L., Mercier, N., and Incerti, S., 2014, Geant4 simulations for sedimentary grains in infinite matrix conditions: The case of alpha dosimetry: Radiation Measurements, v. 70, p. 39–47, <https://doi.org/10.1016/j.radmeas.2014.09.003>.
- Martin, L., Fang, F., Mercier, N., Incerti, S., Grün, R., and Lefrais, Y., 2018, 2D modelling: A Monte Carlo approach for assessing heterogeneous beta dose rate in luminescence and ESR dating: Paper I, theory and verification: Quaternary Geochronology, v. 48, p. 25–37, <https://doi.org/10.1016/j.quageo.2018.07.004>.

- Mayya, Y.S., Morthekai, P., Murari, M.K., and Singhvi, A.K., 2006, Towards quantifying beta microdosimetric effects in single-grain quartz dose distribution: Radiation Measurements, v. 41, no. 7–8, p. 1032–1039, <https://doi.org/10.1016/j.radmeas.2006.08.004>.
- McGregor, I., and Onderdonk, N., 2021, Late Pleistocene rates of rock uplift and faulting at the boundary between the southern Coast Ranges and the western Transverse Ranges in California from reconstruction and luminescence dating of the Orcutt formation: *Geosphere*, v. 17, <https://doi.org/10.1130/GES02274.1>.
- Mejdahl, V., 1972, Dosimetry techniques in thermoluminescence dating: Danish Atomic Energy Commission Risø Report 261, 24 p.
- Mejdahl, V., 1985, Thermoluminescence dating based on feldspars: Nuclear Tracks and Radiation Measurements, v. 10, no. 1/2, p. 133–136, [https://doi.org/10.1016/0735-245X\(85\)90019-5](https://doi.org/10.1016/0735-245X(85)90019-5).
- Mendes, V.R., Sawakuchi, A.O.M., Chiessi, C.F., Giannini, P.C., Rehfeld, K., and Mulitza, S., 2019, Thermoluminescence and optically stimulated luminescence measured in marine sediments indicate precipitation changes over Northeastern Brazil: *Paleoceanography and Paleoclimatology*, v. 34, no. 8, p. 1476–1486, <https://doi.org/10.1029/2019PA003691>.
- Mineli, T.D., Sawakuchi, A.O., Guralnik, B., Lambert, R., Jain, M., Pupim, F.N., DelRio, I., and Guedes, C.C.F., 2021, Variation of luminescence sensitivity, characteristic dose and trap parameters of quartz from rocks and sediments: *Radiation Measurements*, v. 144, <https://doi.org/10.1016/j.radmeas.2021.106583>.
- Morlan, R.E., 1999, Canadian Archaeological Radiocarbon Database: Establishing conventional ages: *Canadian Journal of Archaeology*, v. 23, p. 3–10, [www.jstor.org/stable/41103370](http://www.jstor.org/stable/41103370) (accessed February 2021).
- Moska, P., and Murray, A.S., 2006, Stability of the quartz fast-component in insensitive samples: *Radiation Measurements*, v. 41, p. 878–885, <https://doi.org/10.1016/j.radmeas.2006.06.005>.
- Munyikwa, K., 2000, Cosmic ray contribution to environmental dose rates with varying overburden thickness: *Ancient TL*, v. 18, no. 2, p. 27–34.
- Munyikwa, K., Kinnaird, T.C., and Sanderson, D.C., 2021, The potential of portable luminescence readers in geomorphological investigations: A review: *Earth Surface Processes and Landforms*, v. 46, no. 1, p. 131–150, <https://doi.org/10.1002/esp.4975>.
- Murray, A.S., and Funder, S., 2003, Optically stimulated luminescence dating of a Danish Eemian coastal marine deposit: A test of accuracy: *Quaternary Science Reviews*, v. 22, no. 10–13, p. 1177–1183, [https://doi.org/10.1016/S0277-3791\(03\)00048-9](https://doi.org/10.1016/S0277-3791(03)00048-9).
- Murray, A.S., and Olley, J.M., 2002, Precision and accuracy in the optically stimulated luminescence dating of sedimentary quartz: A status review: *Geochronometria*, v. 21, p. 1–16.
- Murray, A.S., and Roberts, R.G., 1998, Measurement of the equivalent dose in quartz using a regenerative-dose single-aliquot protocol: *Radiation Measurements*, v. 29, no. 5, p. 503–515, [https://doi.org/10.1016/S1350-4487\(98\)00044-4](https://doi.org/10.1016/S1350-4487(98)00044-4).
- Murray, A.S., and Wintle, A.G., 2000, Luminescence dating of quartz using an improved single-aliquot regenerative-dose protocol: *Radiation Measurements*, v. 32, p. 57–73, [https://doi.org/10.1016/S1350-4487\(99\)00253-X](https://doi.org/10.1016/S1350-4487(99)00253-X).
- Murray, A.S., and Wintle, A.G., 2003, The single aliquot regenerative dose protocol: Potential for improvements in reliability: *Radiation Measurements*, v. 37, p. 377–381, [https://doi.org/10.1016/S1350-4487\(03\)00053-2](https://doi.org/10.1016/S1350-4487(03)00053-2).
- Murray, A., Arnold, L.J., Buylaert, J.-P., Guérin, G., Qin, J., Singhvi, A.K., Smedley, R., and Thomsen, K.J., 2021, Optically stimulated luminescence dating using quartz: *National Review*, v. 1, no. 72, p. 1–31, <https://doi.org/10.1038/s43586-021-00068-5>.
- Nathan, R.P., and Mauz, B., 2008, On the dose rate of carbonate-rich sediments for trapped charge dating: *Radiation Measurements*, v. 43, p. 14–25, <https://doi.org/10.1016/j.radmeas.2007.12.012>.
- National Academies of Sciences, Engineering, and Medicine (NASEM), 2020, *A Vision for NSF Earth Sciences 2020–2030: Earth in Time*: Washington, DC, The National Academies Press, 144 p., <https://doi.org/10.17226/25761>.
- Nelson, M.S., and Rittenour, T.M., 2015, Using grain-size characteristics to model soil water content: Application to dose-rate calculation for luminescence dating: *Radiation Measurements*, v. 81, p. 142–149, <https://doi.org/10.1016/j.radmeas.2015.02.016>.
- Nelson, M.S., Gray, H.J., Johnson, J.A., Rittenour, T.M., Feathers, J.K., and Mahan, S.A., 2015, User Guide for Luminescence Sampling in Archaeological and Geological Contexts: *Advances in Archaeological Practice*, v. 3, p. 166–177, <https://doi.org/10.7183/2326-3768.3.2.166>.
- Nelson, M.S., Rittenour, T., and Cornachione, H., 2019, Sampling methods for luminescence dating of subsurface deposits from cores: *Methods and Protocols*, v. 2, no. 4, 15 p, <https://doi.org/10.3390/mps2040088>.
- Neudorf, C.M., Lian, O.B., McIntosh, P.D., Gierich, T.B., and Augustinus, P.C., 2019a, Investigation into the OSL and TT-OSL signal characteristics of ancient (>100 ka) Tasmanian aeolian quartz and its utility as a geochronometer for understanding long-term climate-driven landscape change: *Quaternary Geochronology*, v. 53, <https://doi.org/10.1016/j.quageo.2019.101005>.
- Neudorf, C.M., Quinn, D., and Keen-Zebert, A., 2019b, SPARROW—An open-source laboratory information management system focused on geochronology, in *Proceedings, 13th New World Luminescence Dating Workshop, 5–7 August: Urbana-Champaign, Illinois, University of Illinois*, 46 p.
- Olley, J., Caitcheon, G., and Murray, A., 1998, The distribution of apparent dose as determined by optically stimulated luminescence in small aliquots of fluvial quartz: Implications for dating young sediments: *Quaternary Science Reviews*, v. 17, no. 11, p. 1033–1040, [https://doi.org/10.1016/S0277-3791\(97\)00090-5](https://doi.org/10.1016/S0277-3791(97)00090-5).
- Olley, J.M., Murray, A.S., and Roberts, R.G., 1996, The effects of disequilibria in the uranium and thorium decay chains on burial dose rates in fluvial sediments: *Quaternary Science Reviews*, v. 15, p. 751–760, [https://doi.org/10.1016/0277-3791\(96\)00026-1](https://doi.org/10.1016/0277-3791(96)00026-1).
- Pazzaglia, F.J., Malenda, H., McGavick, M., Raup, C., Carter, M., Berti, C., Mahan, S., Nelson, M., Rittenour, T., Counts, R., Willenbring, J., Germanoski, D., Peters, S., and Holt, W., 2021, River terrace evidence of tectonic processes in the eastern North American plate interior, South Anna River, Virginia: *The Journal of Geology*, <https://doi.org/10.1086/712636>.
- Pérez-Garrido, C., 2020, eM-Age (excel Macro for Age calculation), a new application for luminescence age calculation based on Dose Rate and Age Calculator (DRAC) and Analyst: *Ancient TL*, v. 38, p. 21–24.
- Perić, Z., Adolphi, E.L., Stevens, T., Újvári, G., Zeeden, C., Buylaert, J.-P., Marković, S.B., Hambach, U., Fischer, P., Schmidt, C., Schulte, P., Huay, L., Shuangwen, Y., Lehmkühl, F., Obrecht, I., Veres, D., Thiel, C., Frechen, M., Jain, M., Vött, A., Zöller, L., and Gavrilov, M.B., 2019, Quartz OSL dating of Late Quaternary Chinese and Serbian loess: A cross Eurasian comparison of dust mass accumulation rates: *Quaternary International*, v. 502, p. 30–44, <https://doi.org/10.1016/j.quaint.2018.01.010>.
- Pietsch, T.J., Olley, J.M., and Nanson, G.C., 2008, Fluvial transport as a natural luminescence sensitizer of quartz: *Quaternary Geochronology*, v. 3, no. 4, p. 365–376, <https://doi.org/10.1016/j.quageo.2007.12.005>.
- Porat, N., Duller, G.A.T., Roberts, H.M., and Wintle, A.G., 2009, A simplified SAR protocol for TT-OSL: *Radiation Measurements*, v. 44, no. 5–6, p. 538–542, <https://doi.org/10.1016/j.radmeas.2008.12.004>.
- Prescott, J.R., and Hutton, J.T., 1994, Cosmic ray contributions to dose rates for luminescence and ESR dating: *Radiation Measurements*, v. 23, p. 497–500, [https://doi.org/10.1016/1350-4487\(94\)90086-8](https://doi.org/10.1016/1350-4487(94)90086-8).
- Prescott, J., and Stephan, L., 1982, The contribution of cosmic radiation to the environmental dose for thermoluminescence dating. Latitude, altitude and depth dependences [Council of Europe]: *PACT Journal*, v. 6, p. 17–25.
- Preusser, F., Ramseyer, K., and Schlüchter, C., 2006, Characterisation of low OSL intensity quartz from the New Zealand Alps: *Radiation Measurements*, v. 41, no. 7–8, p. 871–877, <https://doi.org/10.1016/j.radmeas.2006.04.019>.
- Preusser, F., Degering, D., Fuchs, M., Hilgers, A., Kadeireit, A., Klasen, N., Krbetschek, M., Richter, D., and Spencer, J.Q.G., 2008, Luminescence dating: Basics, methods and applications: *Quaternary Science Journal*, v. 57, no. 1–2, p. 95–149.
- Quinn, D., Linzmeier, B., Sundell, K., Gehrels, G., Goring, S., Marcott, S., Meyers, S., Peters, S., Ross, J., Schmitz, M., Singer, B., and Williams, J., 2021, Implementing the Sparrow laboratory data system in multiple subdomains of geochronology and geochemistry: EGU General Assembly 2021, online, 19–30 Apr 2021, EGU21-13832, <https://doi.org/10.5194/egusphere-egu21-13832>.
- Ramsey, K.W., and Baxter, S.J., 1996, Radiocarbon dates from Delaware: A compilation: *Delaware Geological Survey Report of Investigations* 54, p. 1–18.
- Reimann, T., Tsukamoto, S., Naumann, M., and Frechen, M., 2011, The potential of using K-rich feldspars for optical dating of young coastal sediments—a test case from Darss-Zingst peninsula (southern Baltic Sea coast): *Quaternary Geochronology*, v. 6, no. 2, p. 207–222, <https://doi.org/10.1016/j.quageo.2010.10.001>.
- Reinhardt, E.G., Goodman, B.N., Boyce, J.I., López, G.I., van Hengstum, P., Rink, W.J., Mart, Y., and Raban, A., 2006, The tsunami of 13 December AD 115 and the destruction of Herod the Great's harbor at Caesarea Maritima, Israel: *Geology*, v. 34, p. 1061–1064, <https://doi.org/10.1130/G22780A.1>.
- Rhodes, E.J., 2011, Optically stimulated luminescence dating of sediments over the past 200,000 years: *Annual Review of Earth and Planetary Sciences*, v. 39, p. 461–488, <https://doi.org/10.1146/annurev-earth-040610-133425>.
- Rhodes, E.J., Fanning, P.C., and Holdaway, S.J., 2010, Developments in optically stimulated luminescence age control for geochronological sediments and hearths in western New South Wales, Australia: *Quaternary Geochronology*, v. 5, no. 2–3, p. 348–352, <https://doi.org/10.1016/j.quageo.2009.04.001>.
- Ribeiro, L.M.A.L., Sawakuchi, A.O., Wang, H., Sallun Filho, W., and Nogueira, L., 2015, OSL dating of Brazilian fluvial carbonates (tufas) using detrital quartz grains: *Quaternary International*, v. 362, p. 146–156, <https://doi.org/10.1016/j.quaint.2014.11.029>.
- Richards, B.W., 2000, Luminescence dating of Quaternary sediments in the Himalaya and High Asia: A practical guide to its use and limitations for constraining the timing of glaciation: *Quaternary International*, v. 65, p. 49–61, [https://doi.org/10.1016/S1040-6182\(99\)00036-1](https://doi.org/10.1016/S1040-6182(99)00036-1).
- Richter, D., Richter, A., and Dornick, K., 2013, Lexsyg—A new system for luminescence research: *Geochronometria*, v. 40, p. 220–228, <https://doi.org/10.2478/s13386-013-0110-0>.
- Riedesel, S., and Autzen, M., 2020, Beta and gamma dose rate attenuation in rocks and sediment: *Radiation Measurements*, v. 133, <https://doi.org/10.1016/j.radmeas.2020.106295>.
- Riedesel, S., Brill, D., Roberts, H.M., Duller, G.A., Garrett, E., Zander, A.M., King, G.E., Tamura, T., Burow, C., Cunningham, A., and Seeliger, M., 2018, Single-grain feldspar luminescence chronology of historical extreme wave event deposits recorded in a coastal lowland, Pacific coast of central Japan: *Quaternary Geochronology*, v. 45, p. 37–49, <https://doi.org/10.1016/j.quageo.2018.01.006>.
- Riedesel, S., Autzen, M., and Burow, C., 2020, scale\_GammaDose(): Calculate the gamma dose deposited within a sample taking layer-to-layer variations in radioactivity into account (according to Adamiec) Function version 0.1.2, in *Kreutzer, S., Burow, C., Dietze, M., Fuchs, M.C., Schmidt, C., Fischer, M., Friedrich, J., Riedesel, S., Autzen, M., and Mittelstrass, D., 2020, Luminescence: Comprehensive Luminescence Dating Data Analysis. R package version 0.9.10, https://CRAN.R-project.org/package=Luminescence*.
- Rink, W.J., and López, G.I., 2010, OSL-based lateral progradation and aeolian sediment accumulation rates for the Apalachicola Barrier Island complex, North Gulf of Mexico, Florida: *Geomorphology*, v. 123, p. 330–342, <https://doi.org/10.1016/j.geomorph.2010.08.001>.
- Rittenour, T.M., 2008, Luminescence dating of fluvial deposits: Applications to geomorphic, paleoseismic and archaeological research: *Boreas*, v. 37, no. 4, p. 613–635, <https://doi.org/10.1111/j.1502-3885.2008.00056.x>.
- Roberts, H., 2008, The development and application of luminescence dating to loess deposits: A perspective on the past, present and future: *Boreas*, v. 37, no. 4,

- p. 483–507, <https://doi.org/10.1111/j.1502-3885.2008.00057.x>.
- Roberts, H.M., and Duller, G.A., 2004, Standardised growth curves for optical dating of sediment using multiple-grain aliquots: *Radiation Measurements*, v. 38, no. 2, p. 241–252, <https://doi.org/10.1016/j.radmeas.2003.10.001>.
- Roberts, R.G., Galbraith, R.F., Yoshida, H., Laslett, G.M., and Olley, J.M., 2000, Distinguishing dose populations in sediment mixtures: A test of single-grain optical dating procedures using mixtures of laboratory-dosed quartz: *Radiation Measurements*, v. 32, no. 5–6, p. 459–465, [https://doi.org/10.1016/S1350-4487\(00\)00104-9](https://doi.org/10.1016/S1350-4487(00)00104-9).
- Rodnight, H., 2008, How many equivalent dose values are needed to obtain a reproducible distribution?: *Ancient TL*, v. 26, p. 3–9.
- Roos, C.I., Rittenour, T.M., Swetnam, T.W., Loehman, R.A., Hollenback, K.L., Liebmann, M.J., and Rosenstein, D.D., 2020, Fire suppression impacts on fuels and fire intensity in the western US: Insights from archaeological luminescence dating in northern New Mexico: *Fire*, v. 3, no. 3, p. 32, <https://doi.org/10.3390/fire3030032>.
- Rosenzweig, R., and Porat, N., 2015, Evaluation of soil-moisture content for OSL dating using an infiltration model: *Ancient TL*, v. 33, no. 2, p. 10–14.
- Sanderson, D.C., and Murphy, S., 2010, Using simple portable OSL measurements and laboratory characterisation to help understand complex and heterogeneous sediment sequences for luminescence dating: *Quaternary Geochronology*, v. 5, no. 2–3, p. 299–305, <https://doi.org/10.1016/j.quageo.2009.02.001>.
- Sawakuchi, A.O., Blair, M.W., Dewitt, R., Faleiros, F.M., Hyppolito, T., and Guedes, C.C.F., 2011, Thermal history versus sedimentary history: OSL sensitivity of quartz grains extracted from rocks and sediments: *Quaternary Geochronology*, v. 6, no. 2, p. 261–272, <https://doi.org/10.1016/j.quageo.2010.11.002>.
- Sawakuchi, A.O., Jain, M., Mineli, N., Nogueira, L., Bertasoli, D., Jr., Häggi, C., Sawakuchi, H.O., Pupim, F.N., Grohmann, C., Chiessi, C.M., Zabel, M., Mulitza, S., Mazoca, C.E.M., and Cunha, D.F., 2018, Luminescence of quartz and feldspar fingerprints provenance and correlates with the source area denudation in the Amazon River Basin: *Earth and Planetary Science Letters*, v. 492, no. 15, p. 152–162, <https://doi.org/10.1016/j.epsl.2018.04.006>.
- Schiffner, M.B., 1986, Radiocarbon dating and the “old wood” problem: The case of the Hohokam chronology: *Journal of Archaeological Science*, v. 13, no. 1, p. 13–30, [https://doi.org/10.1016/0305-4403\(86\)90024-5](https://doi.org/10.1016/0305-4403(86)90024-5).
- Sellwood, E.L., Guralnik, B., Kook, M., Prasad, A.K., Sohbati, R., Hippe, K., Wallinga, J., and Jain, M., 2019, Optical bleaching front in bedrock revealed by spatially-resolved infrared photoluminescence: *Scientific Reports*, v. 9, 2611, <https://doi.org/10.1038/s41598-019-38815-0>.
- Simms, A.R., DeWitt, R., Kouremenos, P., and Drewry, A.M., 2011, A new approach to reconstructing sea levels in Antarctica using optically stimulated luminescence of cobble surfaces: *Quaternary Geochronology*, v. 6, p. 50–60, <https://doi.org/10.1016/j.quageo.2010.06.004>.
- Singhvi, A.K., and Porat, N., 2008, Impact of luminescence dating on geomorphological and palaeoclimate research in Drylands: *Boreas*, v. 37, p. 536–558, <https://doi.org/10.1111/j.1502-3885.2008.00058.x>.
- Smedley, R.K., and Skirrow, G.K.A., 2020, Luminescence dating in fluvial settings: Overcoming the challenge of partial bleaching, in Herget J., and Fontana A., eds., *Palaeohydrology Traces, Tracks and Trails of Extreme Events: Switzerland*, Springer Nature, p. 155–168, [https://doi.org/10.1007/978-3-030-23315-0\\_8](https://doi.org/10.1007/978-3-030-23315-0_8).
- Smedley, R.K., Buylaert, J.P., and Újvári, G., 2019, Comparing the accuracy and precision of luminescence ages for partially-bleached sediments using single grains of K-feldspar and quartz: *Quaternary Geochronology*, v. 53, <https://doi.org/10.1016/j.quageo.2019.101007>.
- Sohbati, R., Murray, A.S., Jain, M., Buylaert, J.P., and Thomsen, K.J., 2011, Investigating the resetting of OSL signals in rock surfaces: *Geochronometria*, v. 38, no. 3, p. 249–258, <https://doi.org/10.2478/s13386-011-0029-2>.
- Sohbati, R., Murray, A., Lindvold, L., Buylaert, J.P., and Jain, M., 2017, Optimization of laboratory illumination in optical dating: *Quaternary Geochronology*, v. 39, p. 105–111, <https://doi.org/10.1016/j.quageo.2017.02.010>.
- Sontag-González, M., Li, B., O’Gorman, K., Sutikna, T., Jacobs, Z., and Roberts, R.G., 2021, Establishing a pIRIR procedure for De determination of composite mineral grains from volcanic terranes: A case study of sediments from Liang Bua, Indonesia: *Quaternary Geochronology*, v. 65, <https://doi.org/10.1016/j.quageo.2021.101181>.
- Spencer, J.Q., and Sanderson, D.C.W., 2012, Decline in firing technology or poorer fuel resources? High-temperature thermoluminescence (HTTL) archaeothermometry of Neolithic ceramics from Pool, Sanday, Orkney: *Journal of Archaeological Science*, v. 39, no. 12, p. 3542–3552, <https://doi.org/10.1016/j.jas.2012.05.036>.
- Spencer, J.Q., Huot, S., Archer, A.W. and Caldas, M.M., 2019, Testing luminescence dating methods for small samples from very young fluvial deposits: Methods and protocols, v. 2, no. 4, p. 90.
- Steffen, D., Preusser, F., and Schlunegger, F., 2009, OSL quartz age underestimation due to unstable signal components: *Quaternary Geochronology*, v. 4, no. 5, p. 353–362, <https://doi.org/10.1016/j.quageo.2009.05.015>.
- Stevens, T., Buylaert, J.P., Lu, H., Thiel, C., Murray, A., Frechen, M., Yi, S., and Zeng, L., 2016, Mass accumulation rate and monsoon records from Xifeng, Chinese Loess Plateau, based on a luminescence age model: *Journal of Quaternary Science*, v. 31, no. 4, p. 391–405, <https://doi.org/10.1002/jqs.2848>.
- Strebl, D., Brill, D., Richter, J., and Bruckner, H., 2019, Using DRAC in complex geometries—TL dating of heated flints from Taibeh, Jordan: *Quaternary Geochronology*, v. 49, p. 4–7, <https://doi.org/10.1016/j.quageo.2018.07.002>.
- Tamura, T., Cunningham, A.C., and Oliver, T., 2019, Two-dimensional chronostratigraphic modelling of OSL ages from recent beach-ridge deposits, SE Australia: *Quaternary Geochronology*, v. 49, p. 39–44, <https://doi.org/10.1016/j.quageo.2018.03.003>.
- Tecsa, V., Mason, J., Johnson, W., Miao, X., Constantin, D., Radu, S., Magdas, D., Veres, D., Markovic, S.B., and Timar-Gabor, A., 2020, Latest Pleistocene to Holocene loess in the central Great Plains: Optically stimulated luminescence dating and multi-proxy analysis of the enders loess section (Nebraska, USA): *Quaternary Science Reviews*, v. 229, <https://doi.org/10.1016/j.quascirev.2019.106130>.
- Telford, R.J., Heegaard, E., and Birks, H.J., 2004, The intercept is a poor estimate of a calibrated radiocarbon age: *The Holocene*, v. 14, no. 2, p. 296–298, <https://doi.org/10.1191/0959683604hl707fa>.
- Thiel, C., Buylaert, J.P., Murray, A., Terhorst, B., Hofer, I., Tsukamoto, S., and Frechen, M., 2011, Luminescence dating of the Stratzing loess profile (Austria)—Testing the potential of an elevated temperature post-IRSL protocol: *Quaternary International*, v. 234, no. 1–2, p. 23–31, <https://doi.org/10.1016/j.quaint.2010.05.018>.
- Thomas, D.S., and Burrough, S.L., 2016, Luminescence-based dune chronologies in southern Africa: Analysis and interpretation of dune database records across the subcontinent: *Quaternary International*, v. 410, p. 30–45, <https://doi.org/10.1016/j.quaint.2013.09.008>.
- Thomsen, K.J., Murray, A.S., Jain, M., and Bøtter-Jensen, L., 2008, Laboratory fading rates of various luminescence signals from feldspar-rich sediment extracts: *Radiation Measurements*, v. 43, no. 9–10, p. 1474–1486, <https://doi.org/10.1016/j.radmeas.2008.06.002>.
- Tsakalos, E., Christodoulakis, J., and Charalambous, L., 2016, The dose rate calculator (DRc) for luminescence and ESR dating—A Java application for dose rate and age determination: *Archaeometry*, v. 58, p. 347–352.
- Wallinga, J., and Cunningham, A.C., 2015, Luminescence dating, uncertainties and age range, in Rink, W., and Thompson, J., eds., *Encyclopedia of Scientific Dating Methods*: Dordrecht, Netherlands, Springer, p. 440–445, [https://doi.org/10.1007/978-94-007-6304-3\\_197](https://doi.org/10.1007/978-94-007-6304-3_197).
- Wallinga, J., Murray, A., and Wintle, A., 2000, The single-aliquot regenerative-dose (SAR) protocol applied to coarse-grain feldspar: *Radiation Measurements*, v. 32, no. 5–6, p. 529–533, [https://doi.org/10.1016/S1350-4487\(00\)00091-3](https://doi.org/10.1016/S1350-4487(00)00091-3).
- Watanuki, T., Murray, A.S., and Tsukamoto, S., 2005, Quartz and polymineral luminescence dating of Japanese loess over the last 0.6 Ma: Comparison with an independent chronology: *Earth and Planetary Science Letters*, v. 240, no. 3–4, p. 774–789, <https://doi.org/10.1016/j.epsl.2005.09.027>.
- Williams, A.N., Ulm, S., Smith, M., and Reid, J., 2014, AustArch: A database of <sup>14</sup>C and non-<sup>14</sup>C ages from archaeological sites in Australia—composition, compilation and review (data paper): *Internet Archaeology*, v. 36, <https://doi.org/10.1141/ia.36.6>.
- Williams, J.W., Grimm, E.G., Blois, J., Charles, D.F., Davis, E., Goring, S.J., Graham, R., Smith, A.J., Anderson, M., Arroyo-Cabral, J., Ashworth, A.C., Betancourt, J.L., Bills, B.W., Booth, R.K., Buckland, P., Curry, B., Giesecke, T., Hausmann, S., Jackson, S.T., Latorre, C., Nichols, J., Purdum, T., Roth, R.E., Stryker, M., and Takahara, H., 2018, The Neotoma Paleocology Database: A multi-proxy, international community-curated data resource: *Quaternary Research*, v. 89, p. 156–177, <https://doi.org/10.1017/qua.2017.105>.
- Willmes, C., 2016, CRC806-Database: A semantic e-Science infrastructure for an interdisciplinary research centre [Ph.D. thesis]: Cologne, Germany, University of Cologne, 311 p.
- Willmes, C., Viehberg, F., Lopez, S.E., and Bareth, G., 2018, CRC806-KB: A semantic MediaWiki based collaborative knowledge base for an interdisciplinary research project: *Data (København)*, v. 3, p. 44, <https://doi.org/10.3390/data3040044>.
- Wintle, A.G., 1973, Anomalous fading of thermoluminescence in mineral samples: *Nature*, v. 245, p. 143–144, <https://doi.org/10.1038/245143a0>.
- Wintle, A.G., 1997, Luminescence dating: Laboratory procedures and protocols: *Radiation Measurements*, v. 27, no. 5–6, p. 769–817, [https://doi.org/10.1016/S1350-4487\(97\)00220-5](https://doi.org/10.1016/S1350-4487(97)00220-5).
- Wintle, A.G., 2008, Fifty years of luminescence dating: *Archaeometry*, v. 50, no. 2, p. 276–312, <https://doi.org/10.1111/j.1475-4754.2008.00392.x>.
- Wintle, A.G., and Adamiec, G., 2017, Optically stimulated luminescence signals from quartz: A review: *Radiation Measurements*, v. 98, p. 10–33, <https://doi.org/10.1016/j.radmeas.2017.02.003>.
- Wintle, A.G., and Murray, A.S., 2006, A review of quartz optically stimulated luminescence characteristics and their relevance in single-aliquot regeneration dating protocols: *Radiation Measurements*, v. 41, no. 4, p. 369–391, <https://doi.org/10.1016/j.radmeas.2005.11.001>.
- Wintle, A.G., Aitken, M.J., and Huxtable, J., 1971, Abnormal thermoluminescence fading characteristics, Proceedings of the Third International Conference on Luminescence Dosimetry, held at the Danish Atomic Energy Commission Research Establishment, Risø, October 1971: *Danish Atomic Energy Commission Risø Report* 249, p. 105–131.
- Yoshida, H., Roberts, R.G., Olley, J.M., Laslett, G.M., and Galbraith, R.F., 2000, Extending the age range of optical dating using single ‘supergrains’ of quartz: *Radiation Measurements*, v. 32, no. 5–6, p. 439–446, [https://doi.org/10.1016/S1350-4487\(99\)00287-5](https://doi.org/10.1016/S1350-4487(99)00287-5).
- Zhang, J., and Li, S.H., 2020, Review of the Post-IRSL dating protocols of K-feldspar: *Methods and Protocols*, v. 3, no. 7, 19 p., <https://doi.org/10.3390/mps3010007www.mdpi.com/journal/mps>.
- Zeeden, C., Dietze, M., and Kreutzer, S., 2018, Discriminating luminescence age uncertainty composition for a robust Bayesian modelling: *Quaternary Geochronology*, v. 43, p. 30–39, <https://doi.org/10.1016/j.quageo.2017.10.001>.

SCIENCE EDITOR: BRAD S. SINGER

MANUSCRIPT RECEIVED 1 DECEMBER 2021

REVISED MANUSCRIPT RECEIVED 21 FEBRUARY 2022

MANUSCRIPT ACCEPTED 13 MAY 2022

Printed in the USA